International Journal of Mathematical Archive-7(4), 2016, 71-98
Available online through www.ijma.info ISSN 2229 – 5046

FINITE ELEMENT ANALYSIS OF DOUBLE-DIFFUSIVE HEAT TRANSFER FLOW IN RECTANGULAR DUCT WITH THERMO-DIFFUSION AND RADIATION EFFECTS UNDER INCLINED MAGNETIC FIELD

B. UMA DEVI*[1], Dr. R. BHUVANA VIJAYA[2]

[1]Department of Mathematics, SBIT Khammam, Telangana, India.

[2]Department of Mathematics, JNTUA, Anantapuramu, (A.P.), India.

(Received On: 10-02-16; Revised & Accepted On: 13-04-16)

ABSTRACT

An investigation has been carried out to find the influence of the thermal radiation and thermo-diffusion on convective heat and mass transfer flow of a viscous chemically reacting and electrically fluid through a porous medium in a rectangular duct under inclined magnetic field. By using Galerkin finite element method the equations governing the flow, heat and mass transfer have been solved with three nodded triangular elements. The effects of various parameters like soret parameter Sr, chemical reaction parameter γ, radiation parameter N_1, Eckert number Ec and inclination of the magnetic field the temperature α_1, concentration C, the rate of heat and mass transfer have been depicted. It is noticed that the actual temperature and concentration reduces at the vertical levels x=1/3, 2/3 and at horizontal level y=2h/3, while reduces at the horizontal level y=h/3 with increase in radiation parameter N_1

Keywords: *Chemical reaction, Dissipation, Inclined magnetic field, Radiation effect, Rectangular Duct, Soret effect.*

NOMENCLATURE

H_0	Applied Magnetic Field
C	Concentration of the Solute
C_0	Reference Concentration
C_h	Concentration of the solute at hot wall
C_c	Concentration of the Solute at Cold Wall
C_p	Specific heat at constant pressure [J/kg K]
C_w	Concentration of the solute at the plate
D_m	Molecular diffusivity
Ec	Eckert Number $= \left(\frac{a^4}{\mu k k_f \Delta T} \right)$
G	Grashof number $= (\frac{g\beta(T_h - T_c)a^3}{\nu^2})$
k	Permeability of porous medium[m^2]
k_f	Thermal conductivity of the fluid [W/m K]
B_r	Mean absorption coefficient
M^2	Magnetic Field Parameter $= \frac{\sigma \mu_e^2 H_o^2 L^2}{\nu^2}$
N	Buoyancy ratio $= \frac{\beta^*(C_h - C_c)}{\beta(T_h - T_c)}$
Nu	Nusselt Number
P	Prandtl Number $=\mu C_p / K_f$

Corresponding Author: B. Uma Devi*[1]
[1]Department of Mathematics, SBIT Khammam, Telangana, India.

Q Additional heat source
q_r Radiative heat flux
r′ Chemical reaction constant
Sc Scmidt parameter $= \frac{\nu}{D}$
Sh herwood Number
Ra Rayleigh Number $= \frac{\beta g(T_g - T_c)ka}{\nu^2}$
Sr Soret parameter $= \frac{k_{11}\beta^{\bullet}}{\nu\beta}$
H Step function
N_1 Radiation parameter $= \frac{4\sigma^{\bullet}T_e^3}{3\beta_R k_f}$
T Temperature of the fluid in the boundary [^oC]
T_h Temperature of the field at the hot wall [^oC]
T_c Temperature of the field at the cold wall[^oC]
T_w Wall temperature [^oC]
(u,v) Velocity components[ms^{-1}]
(x,y) Cartesian coordinates[m]

GREEK SYMBOLS

γ Chemical reaction parameter
β_0 Coefficient of thermal expansion [K^{-1}]
β* Coefficient of concentration expansion
μ viscosity of the fluid [kg m^{-1} s^{-1}]
υ Kinematic Viscosity [m^2s^{-1}]
μ_e Magnetic permeability
σ* Stefan – Boltzman constant parameter
ρ Density of the fluid [kgm^{-3}]
ϕ Non dimensional concentration
θ Non dimensional temperature
α Heat Source parameter $=Qa^z/k_f$
α_1 Angle of inclination
Ψ Stream function [m^2s^{-1}]

1. INTRODUCTION

Natural convection is of great importance in many applications of industries. Convection plays an authoritative role in crystal growth in which it affects the composition of fluid-phase and temperature at the phase interface whose consequence results in a single crystal since poor crystal quality is due to turbulence. It is the base in modern electronics industry to produce pure and perfect crystals that are used to make lasers rods, transistors, infrared detectors, microwave devices, memory devices, and IC's (integrated circuits). Natural convection harmfully affects local growth conditions and increases the overall transport rate.

Convective heat transfer in a porous duct which is rectangular and the vertical walls are maintained at two different temperatures and the horizontal walls being insulated is a problem which has grabbed interest by several authors. Verschoor and Greebler [1] have investigated heat transfer in enclosures experimentally. From the literature we find that that the influence of viscous dissipation on heat transfer has been examined for different shapes. The influence of viscous dissipation and radiation on transient MHD free convection flow past vertical plate in porous medium has been analyzed by Verschoor *et al.* [1]. Kamotoni *et al.* [2] have conducted experiments on mass transfer with height and length ratio lies between0.13-0.55 that is filled with a fluid where the combined buoyancy effects are controlled by the buoyancy due to differences in concentration. The combination of temperature and concentration gradients in the fluid will result in buoyancy-driven flows. This has a significant effect on the solidification process in a binary system. Simultaneous heat and mass transfer give rise complex fluid motion referred as double-diffusive convection, which occurs in many scientific fields such as geology, astrophysics, and oceanography. Ostrach [3] and Viskanta *et al.* [4] have delineated entire reviews on the subject. The scale analysis of heat and mass transfer within spaces with horizontal, combined temperature and concentration gradients has been discussed by Bejan[5]. The experimental

studies with thermo-solutal convection in rectangular ducts were discussed by Lee *et al.* [6]. Lee and Hyun [7] delineated numerical solutions for transient double-diffusive convection in a rectangular duct with buoyancy forces agrees with the experimental results. Other related numerical studies marketing with double-diffusive natural convection in cavities were considered by Ranganathan and Viskanta [8], Trevisan and Bejan [9, 10], Beghein *et al.* [11] and Nishimura *et al.* [12].

Electrically conducting fluids under the influence of a magnetic field have been broadly studied in many applications such as crystal growth. Oreper and Szekely [13] have found that the presence of a magnetic field can overcome natural convection currents and that the factors in deciding the quality of the crystal. Ozone and Maruo [14] have inspected magnetic and gravitational natural convection of melted silicon-two dimensional numerical estimations needed for the rate of heat transfer. Garandet *et al.* [15] and Alchaar *et al*. [16] have treated free convection MHD heat transfer in a rectangular duct. Rudraiah *et al.* [17] and Al-Najem *et al.* [18] have discussed the influences of a magnetic field on free convection in a rectangular fold. Mamun *et al.* [19] have inspected natural convection in a porous trapezoidal fold with magneto hydrodynamic effect. The dominating equations are solved by using Galerkin weighted residual method of finite element formulation. It is found that with developing Ha, the diffusive heat transfer become important even though the changed Rayleigh number increases. Rahaman *et al.* [20] have carried out the conjugate influence of joule heating and magneto hydrodynamic on double diffusive mixed convection in a horizontal channel with an open cavity. Homogenous flows are lay down all through the channel. The temperature, concentration, average nusselt and Sherwood number have been inspected for different values of Hartmann number, Lewis number, Joule heating, Buoyancy ratio and Richardson number. Rahman *et al.* [21] have inspected double diffusive natural convection in a triangular shaped solar collector. Considering the isothermal and iso-concentration boundary conditions of absorber and covers of collectors, the two dimensional equations have been solved by finite element method. The effect of buoyancy ratio and thermal Rayleigh number on local and mean heat and mass transfer rates has been examined. Ching *et al.* [22] have carried out numerical investigation on mixed convective heat and mass transfer in a right triangular duct. The effect of Richardson number, buoyancy ratio and the direction of the sliding wall motion on the flow, temperature, rate of heat and mass transfer has been examined. It strengthens with rise in the buoyancy ratio. The flow and temperature can be controlled by the direction of the sliding wall motion. Rahman *et al.* [23] have examined natural convection influences on heat and mass transfer in a bending triangular cavity using jagged shaped bottom wall by using finite element method. As Br increases, the average Nusselt number and Sherwood Number also strengthens. With increase in Le, Sherwood number strengthens and an average Nusselt number reduces. Oztop *et al.* [24] have studied the thermal and dynamical behavior of fluid in fold with two isothermal semi-circular heaters. The top wall and the flat surfaces of the bottom wall are adiabatic along the vertical walls that are kept at lower temperature than that with the semicircular heaters. The corresponding equations are solved by the Galerkin weighted residual finite element method. The difference between the semi-circular heaters has an effect over the heat and fluid flow fields. Hartmann number has a very bad effect on heat transfer.

Natural convection heat transfer that is induced by internal heat generation has recently received substantial attention because of various applications. Such applications even include underground disposal of radioactive waste materials, heat removal from nuclear fuel debris, exothermic chemical reactions in packed-bed reactor and storage of foodstuff (see, for instance, [25]-[29]). Acharya and Goldstein [30] studied numerically two-dimensional natural convection of air in an externally heated vertical or inclined square box with uniformly distributed internal energy sources. The results of the above showed two distinct flow pattern systems confiding on the ratio of the internal to the external Raleigh numbers. The average heat flux ratio along the cold wall increased with decreasing internal Rayleigh numbers and increasing external Rayleigh numbers. Latterly, Churbanov *et al.* [31] studied numerically unsteady natural convection of a heat generating fluid in a vertical rectangular fold with the walls being isothermal or adiabatic. The governing non-linear equations are solved using finite-difference scheme in the two-dimensional stream function with velocity formulation. Other related works regarding temperature-dependent heat generation influences can be found in the papers by Vajravelu and Nayfeh [32] and Chamkha [33].

A lot of useful work has been carried out to know about natural convection in porous cavity. In spite of these studies heat transfer in porous cavity, the combined influence of viscous dissipation and radiation on porous medium filled inside a square cavity has not gained proper interest. The convective heat transfer through a porous medium in a rectangular cavity with heat sources and dissipation under diverse conditions have been carried out by several researchers [34-37]. Ranga Reddy [38] has conferred when the side walls of the rectangular cavity are differentially heated using Brinkman model, natural convective heat and mass transfer flow equations are solved with the help of Galerkin finite element method. The effect of thermo-diffusion on convective heat transfer flow of a viscous fluid through a porous medium with buoyancy forces in rectangular duct has been studied by Sivaiah [39].

Santhi *et al.* [40] has examined double diffusive flow in a rectangular cavity with the help of Darcy model. She has examined the influence of dissipation and radiation on the double diffusive flow of a viscous fluid in the rectangular cavity. Chamka *et al.* [41] have examined the Hydro magnetic double-diffusive convection in a rectangular duct with opposing buoyancy forces.

2. MATHEMATICAL FORMULATION

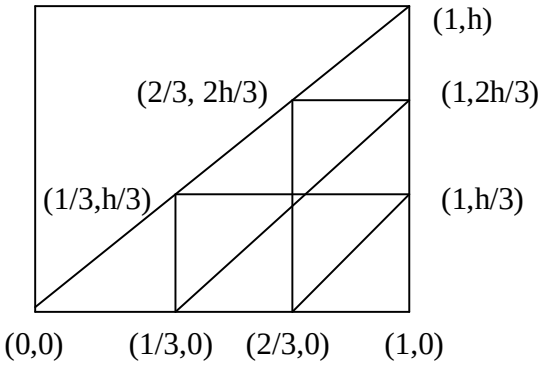

Fig. 1: Rectangular Duct.

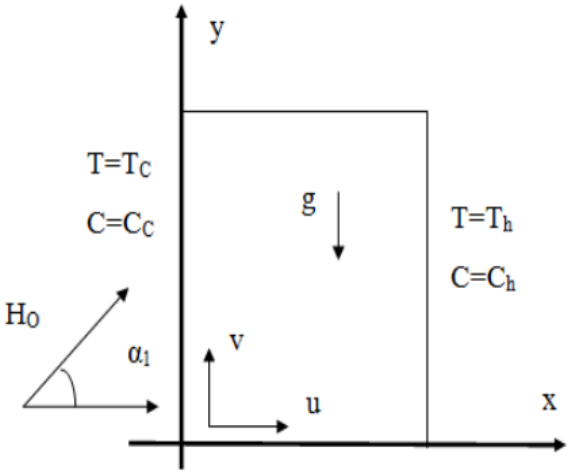

Fig. 2: Physical Configuration and Co-ordinate system.

We consider the mixed convective heat and mass transfer flow of a viscous incompressible fluid in a saturated porous medium confined in the rectangular duct (Fig.2) whose base length is a and height b. The base and top walls of the duct are maintained at constant heat flux. By choosing the Cartesian coordinate system O (x, y) as origin on the base of the duct and is parallel to x-axis.

The equations of motion are

$$\frac{\partial u'}{\partial x'}+\frac{\partial v'}{\partial y'}=0 \tag{1}$$

$$\frac{\partial u'}{\partial y'}\mu\frac{\partial v'}{\partial x'}x=\frac{k}{}\frac{\partial(\rho' g)}{\partial\ '}+\left(\frac{\sigma\mu_e^2 H_o^2}{(\mu/\rho)}\right)\left(-\frac{\partial u'}{\partial\ '}\underset{y}{\text{Sin}^2}\alpha_1+2\frac{\partial v'}{\partial\ '}\text{Sin}(\alpha_1)\underset{x}{\text{Cos}}(\alpha_1)+\frac{\partial v'}{\partial\ '}\text{Cos}^2(\alpha_1)\right) \tag{2}$$

$$\rho_\sigma C_p\left(u'\frac{\partial T'}{\partial x'}+v'\frac{\partial T'}{\partial y'}\right)=k_f\left(\frac{\partial^2 T'}{\partial x'^2}+\frac{\partial^2 T'}{\partial y'^2}\right)+Q(T_0-T')+\mu(u'^2+v'^2)-\frac{\partial(q_r)}{\partial x'} \tag{3}$$

$$\left(u'\frac{\partial C'}{\partial x'}+v'\frac{\partial C'}{\partial y'}\right)=D_m\left(\frac{\partial^2 C'}{\partial x'^2}+\frac{\partial^2 C'}{\partial y'^2}\right)+\frac{D_m k_T}{T_m}\left(\frac{\partial^2 T'}{\partial x'^2}+\frac{\partial^2 T'}{\partial y'^2}\right)-\gamma'(C'-C_o)$$

$$\rho'=\rho_0\left\{1-\beta_0(T'-T_0)-\beta^{\bullet}(C'-C_0)\right\} \tag{4}$$

$$T_0=\frac{T_h+T_c}{2},C_0=\frac{C_h+C_c}{2}$$

Where u′ and v′ are Darcy velocities along θ(x, y) direction. T′, C′, p′, ρ′, and g′ are the temperature, concentration, pressure, density and acceleration due to gravity. H_o is the magnetic field strength.

The boundary conditions are (fig. 2)

$u' = v' = 0$ on the boundary of the duct

$T' = T_c$, $C' = C_c$ on the side wall to the left

$T' = T_h$, $C' = C_h$ on the side wall to the right (5)

$\frac{\partial T'}{\partial y'} = 0$, $\frac{\partial C'}{\partial y'} = 0$ on the top (y = 0) and bottom

$u' = v' = 0$ walls (y = 0) which are insulated.

Following Rosseland approximation for radiation

$$q_r = \frac{4\sigma^*}{3\beta_R}\frac{\partial T'^4}{\partial y}$$

Expanding T'^4 in Taylor's series about T_e and neglecting higher order terms

$$T'^4 \cong 4T_e^3 T - 3T_e^4$$

On introducing the dimensionless variables

$x' = ax$; $y' = by$; $c = b/a$

$u' = (\nu/a)\,u$; $v' = (\nu/a)v$; $p' = (\nu^2\rho/a^2)p$

$T' = T_c + \theta\,(T_h - T_c)$; $C' = C_c + \phi\,(T_h - T_c)$ (6)

The equations in the dimensionless form are

$$\frac{\partial u}{\partial y} - \frac{\partial v}{\partial x} = Ra\left(\frac{\partial \theta}{\partial x} + N\frac{\partial \varphi}{\partial x}\right) + M^2\left(-\frac{\partial u}{\partial y}\mathrm{Sin}^2\alpha_1 + 2\frac{\partial v}{\partial y}\mathrm{Sin}(\alpha_1)\mathrm{Cos}(\alpha_1) + \frac{\partial v}{\partial x}\mathrm{Cos}^2(\alpha_1)\right) \quad (7)$$

$$P\left(u\frac{\partial \theta}{\partial x} + v\frac{\partial \theta}{\partial y}\right) = \left(1 + \frac{4N_1}{3}\right)\left(\frac{\partial^2\theta}{\partial x^2} + \frac{\partial^2\theta}{\partial y^2}\right) - \alpha\theta + \mu(u^2 + v^2) \quad (8)$$

$$Sc\left(u\frac{\partial \phi}{\partial x} + v\frac{\partial \phi}{\partial y}\right) = \left(\frac{\partial^2\phi}{\partial x^2} + \frac{\partial^2\phi}{\partial y^2}\right) + \frac{ScSr}{N}\left(\frac{\partial^2\theta}{\partial x^2} + \frac{\partial^2\theta}{\partial y^2}\right) - \gamma\phi \quad (9)$$

Following (1) we introduce the stream function ψ as

$$u = \frac{\partial \psi}{\partial y};\quad v = -\frac{\partial \psi}{\partial x} \quad (10)$$

Using (10) the equations (7-9) reduces to

$$\left(\frac{\partial^2\psi}{\partial x^2} + \frac{\partial^2\psi}{\partial y^2}\right) = -Ra\left(\frac{\partial \theta}{\partial x} + N\frac{\partial \varphi}{\partial x}\right) + M^2\left(\frac{\partial^2\psi}{\partial y^2}\mathrm{Sin}^2\alpha_1 + 2\frac{\partial^2\psi}{\partial x\partial y}\mathrm{Sin}(\alpha_1)\mathrm{Cos}(\alpha_1) + \frac{\partial^2\psi}{\partial x^2}\mathrm{Cos}^2(\alpha_1)\right) \quad (11)$$

$$P\left(\frac{\partial \psi}{\partial y}\ \frac{\partial \theta}{\partial x} - \frac{\partial \psi}{\partial x}\ \frac{\partial \theta}{\partial y}\right) = \left(1 + \frac{4N_1}{3}\right)\left(\frac{\partial^2\theta}{\partial x^2} + \frac{\partial^2\theta}{\partial y^2}\right) - \alpha\theta + \mu\left(\left(\frac{\partial \psi}{\partial x}\right)^2 + \left(\frac{\partial \psi}{\partial y}\right)^2\right) \quad (12)$$

$$Sc\left(\frac{\partial \psi}{\partial y}\ \frac{\partial \phi}{\partial x} - \frac{\partial \psi}{\partial x}\ \frac{\partial \phi}{\partial y}\right) = \left(\frac{\partial^2\phi}{\partial x^2} + \frac{\partial^2\phi}{\partial y^2}\right) + \frac{ScSr}{N}\left(\frac{\partial^2\theta}{\partial x^2} + \frac{\partial^2\theta}{\partial y^2}\right) \quad (13)$$

where

$G = \frac{g\beta(T_h - T_c)a^3}{\nu^2}$ (Grashof number), $P = \mu\,C_p / k_f$ (Prandtl number)

$\alpha = Qa^2/k_f$ (Heat source parameter), $Ra = \frac{\beta g(T_g - T_c)ka}{\nu^2}$ (Rayleigh Number)

$N_1 = \frac{4\sigma^* T_e^3}{3\beta_R k_f}$ (Radiation parameter), $Sc = \frac{\nu}{D_m}$ (Schmidt Number)

$Sr = \frac{k_{11}\beta^{\bullet}}{\nu\beta}$ (Soret parameter), $N = \frac{\beta^{*}(C_h - C_c)}{\beta(T_h - T_c)}$ (Buoyancy ratio)

$M^2 = \frac{\sigma\mu_e^2 H_o^2 L^2}{\nu^2}$ (Magnetic parameter), $Ec = \left(\frac{a^4}{\mu k k_f \Delta T}\right)$ (Eckert number)

The boundary conditions are

$$\frac{\partial\psi}{\partial x} = 0, \frac{\partial\psi}{\partial y} = 0 \ on \quad x = 0 \ \& 1 \tag{14}$$

$$\theta = 0 \quad \phi = 0 \quad on \quad x = 0$$
$$\theta = 1 \quad \phi = 1 \quad on \quad x = 1 \tag{15}$$

3. METHOD OF SOLUTION

3.1 Finite Element Method:

In this method, the domain is partitioned into a finite number of three node triangular elements (fig. 1). The element equations are derived using finite element method. The corresponding variation formulation results in a 3 x 3 matrix equations. The stiffness matrices in terms of unknown local nodal values of each element are put together in terms of global nodal values making use of inter element continuity conditions giving rise to global matrix equation.

In each case there are r distinct global nodes in the finite element domain and f_p (p = 1, 2,…r) is the global nodal values of any unknown f defined over the domain then

$$f = \sum_{i=1}^{8} \sum_{p=1}^{r} f_p \ \Phi_p^i ,$$

where the first summation denotes summation over s elements and the second one represents summation over the independent global nodes and

$\Phi_p^i = N_N^i$, if p is one of the local nodes say k of the element e_i

= 0, otherwise.

f_p' s are determined from the global matrix equation. Applying finite element analysis to the equations (11) – (13) subjected to the conditions (14) – (15).

Assuming ψ^i , θ^i and ϕ^i to be the approximate values of ψ ,θ and ϕ in an element θ_i.

$$\psi^i = N_1^i\psi_1^i + N_2^i\psi_2^i + N_3^i\psi_3^i \tag{16}$$

$$\theta^i = N_1^i\theta_1^i + N_2^i\theta_2^i + N_3^i\theta_3^i \tag{17}$$

$$\phi^i = N_1^i\iota_1^i + N_2^i\phi_2^i + N_3^i\phi_3^i \tag{18}$$

On substituting (16) – (18) in (12) – (13), the corresponding errors are

$$E_1^i = \left(1 + \frac{4}{3N_1}\right)\frac{\partial^2\theta^i}{\partial x^2} + \frac{\partial^2\theta^i}{\partial y^2} - p\left(\frac{\partial\psi^i}{\partial y}\frac{\partial\theta^i}{\partial x} + \frac{\partial\psi^i}{\partial x}\frac{\partial\theta^i}{\partial y}\right) - \alpha\theta + Ec\left(\left(\frac{\partial\psi^i}{\partial x}\right)^2 + \left(\frac{\partial\psi^i}{\partial y}\right)^2\right) \tag{19}$$

$$E_2^i = \frac{\partial^2\theta^i}{\partial x^2} + \frac{\partial^2\theta^i}{\partial y^2} - Sc\left(\frac{\partial\psi^i}{\partial y}\frac{\partial\theta^i}{\partial x} + \frac{\partial\psi^i}{\partial x}\frac{\partial\theta^i}{\partial y}\right) + \frac{ScSr}{N}\left(\frac{\partial^2\theta^i}{\partial x^2} + \frac{\partial^2\theta^i}{\partial y^2}\right) - \gamma\phi \tag{20}$$

By making these errors orthogonal to shape functions we get

$$\int_{e_i} E_1^i N_k^i d\Omega = 0, \qquad \int_{e_i} E_2^i N_k^i d\Omega = 0,$$

$$\int_{e_i} N_k^i \left(1 + \frac{4}{3N_1}\right)\left(\frac{\partial^2\theta^i}{\partial x^2} + \frac{\partial^2\theta^i}{\partial y^2}\right) - p\left(\frac{\partial\psi^i}{\partial y}\frac{\partial\theta^i}{\partial x} + \frac{\partial\psi^i}{\partial x}\frac{\partial\theta^i}{\partial y}\right) - \alpha\theta + Ec\left(\left(\frac{\partial\psi^i}{\partial x}\right)^2 + \left(\frac{\partial\psi^i}{\partial y}\right)^2\right) d\Omega = 0 \tag{21}$$

$$\int_{e_i}\left(\left(\frac{\partial^2\theta^i}{\partial x^2}+\frac{\partial^2\theta^i}{\partial y^2}\right)-Sc\left(\frac{\partial\psi^i}{\partial y}\frac{\partial\theta^i}{\partial x}+\frac{\partial\psi^i}{\partial x}\frac{\partial\theta^i}{\partial y}\right)\frac{ScSr}{N}\left(\frac{\partial^2\theta^i}{\partial x^2}+\frac{\partial^2\theta^i}{\partial y^2}\right)-\gamma\phi\right)d\Omega=0 \tag{22}$$

Applying Green's theorem to (21) & (22) without affecting ψ terms and obtain

$$\int_{e_i}N_k^i\left\{\left(1+\frac{4}{3N_1}\right)\frac{\partial N_k^i}{\partial x}\frac{\partial\theta^i}{\partial x}+\frac{\partial N_k^i}{\partial y}\frac{\partial\theta^i}{\partial y}-PN_k\left(\frac{\partial\psi^i}{\partial y}\frac{\partial\theta^i}{\partial x}+\frac{\partial\psi^i}{\partial x}\frac{\partial\theta^i}{\partial y}\right)-\alpha\theta^i+Ec\left(\left(\frac{\partial\psi^i}{\partial x}\right)^2+\left(\frac{\partial\psi^i}{\partial y}\right)^2\right)\right\}d\Omega$$

$$=\int_{\Gamma_i}N_k^i\left(\left(\frac{\partial\theta^i}{\partial x}+Du\frac{\partial\phi^i}{\partial x}\right)n_x+\left(\frac{\partial\theta^i}{\partial y}+Du\frac{\partial\phi^i}{\partial y}\right)n_y\right)d\Gamma_i \tag{23}$$

$$\int_{e_i}N_k^i\left\{\frac{\partial N_k^i}{\partial x}\frac{\partial\theta^i}{\partial x}+\frac{\partial N_k^i}{\partial y}\frac{\partial\theta^i}{\partial y}-Sc^iN_k\left(\frac{\partial\psi^i}{\partial y}\frac{\partial\theta^i}{\partial x}+\frac{\partial\psi^i}{\partial x}\frac{\partial\theta^i}{\partial y}\right)+\frac{ScSr}{N}\left(\frac{\partial N_k^i}{\partial x}\frac{\partial\theta^i}{\partial x}+\frac{\partial N_k^i}{\partial y}\frac{\partial\theta^i}{\partial y}\right)-\gamma\phi^i\right\}d\Omega$$

$$=\int_{\Gamma_i}N_k^i\left(\left(\frac{\partial\phi^i}{\partial x}+\frac{ScSr}{N}\frac{\partial\theta^i}{\partial x}\right)n_x+\left(\frac{\partial\phi^i}{\partial y}+\frac{ScSo}{N}\frac{\partial\theta^i}{\partial x}y\right)n_y\right)d\Gamma_i \tag{24}$$

where Γ_I is the boundary of e_i.

Putting the approximate values in (23) & (24) we get

$$\sum_1\int_{e_i}\left(1+\frac{4N}{3}\right)\frac{\partial N_k^i}{\partial x}\frac{\partial N_L^i}{\partial x}+\frac{\partial N_k^i}{\partial y}\frac{\partial N_L^i}{\partial y}-P\sum_1\psi_m^i\left(\frac{\partial N_m^i}{\partial x}\frac{\partial N_L^i}{\partial x}+\frac{\partial N_m^i}{\partial y}\frac{\partial N_L^i}{\partial y}\right)d\Omega$$

$$-\alpha\sum\theta^i\int_{e_i}NN_k^l+Ec\int_{e_i}\left(\left(\frac{\partial\psi^i}{\partial y}\right)^2+\left(\frac{\partial\psi^i}{\partial x}\right)^2\right)d\Omega$$

$$=\int_{\Gamma_i}N_k^i\left(\frac{\partial\theta^i}{\partial x}\;\;n_x+\frac{\partial\theta^i}{\partial y}n_y\right)d\Gamma_i=Q_k^i,\ (l,\,m,\,k=1,2,3) \tag{25}$$

$$\sum_1\int_{e_i}\phi^i\left(\frac{\partial N_k^i}{\partial x}\frac{\partial\theta^i}{\partial x}+\frac{\partial N_k^i}{\partial y}\frac{\partial\theta^i}{\partial y}\right)-Sc\sum_1\psi_m^i\int_{e_i}\left(\frac{\partial N_m^i}{\partial y}\frac{\partial N_L^i}{\partial x}+\frac{\partial N_m^i}{\partial x}\frac{\partial N_L^i}{\partial y}\right)d\Omega$$

$$+\frac{ScSr}{N}\sum\theta^i\int_{e_i}\left(\frac{\partial N_k^i}{\partial x}\frac{\partial N_L^i}{\partial x}+\frac{\partial N_k^i}{\partial y}\frac{\partial N_L^i}{\partial y}\right)d\Omega-\gamma\sum\phi^i\int_{\Omega_i}N_k^iN_L^id\Omega$$

$$=\int_{\Gamma_i}N_k^i\left(\left(\frac{\partial\phi^i}{\partial x}+\frac{ScSr}{N}\frac{\partial\theta^i}{\partial x}\right)n_x+\left(\frac{\partial\phi^i}{\partial y}+\frac{ScSr}{N}\frac{\partial\theta^i}{\partial x}y\right)n_y\right)d\Gamma_i=Q_i^c,\left(l,\,m,\,k=1,\,2,\,3\right) \tag{26}$$

where

$Q_k^i=Q_{k1}^i+Q_{k2}^i+Q_{k3}^i, Q_k^i$'s being the values of Q_k^i on the sides s = (1, 2, 3) of the element e_i. The sign of Q_k^i's depends on the direction of the outward normal w.r.to the element. Choosing different N_k^i's as shape functions and following the same procedure we obtain matrix equations for three unknowns (Q_p^i) viz.

$$(Q_p^i)(\theta_p^i)=(Q_k^i) \tag{27}$$

where (Q_p^i) is a 3 x 3 matrix, $(\theta_p^i),(Q_k^i)$ are column matrices.

Repeating the above process with each of s elements, we obtain sets of such matrix equations.

On substituting (16) – (18) in (11) the corresponding error is

$$E_3^i = \left(\frac{\partial^2\psi}{\partial x^2} + \frac{\partial^2\psi}{\partial y^2}\right) + Ra\left(\frac{\partial\theta}{\partial x} + N\frac{\partial\varphi}{\partial x}\right) - M^2\left(\frac{\partial^2\psi}{\partial y^2}\mathrm{Sin}^2\alpha_1 + 2\frac{\partial^2\psi}{\partial x\partial y}\mathrm{Sin}(\alpha_1)\mathrm{Cos}(\alpha_1) + \frac{\partial^2\psi}{\partial x^2}\mathrm{Cos}^2(\alpha_1)\right)d\Omega_i \quad (28)$$

and following the Variation formulation we get

$$\int_\Omega E_3^i\psi_j^i d\Omega = 0 \quad (29)$$

Applying Green's theorem to the surface integral (29) without affecting θ terms.

$$\int_\Omega \left(\begin{array}{l} \left(\frac{\partial N_k^i}{\partial x} \quad \frac{\partial\psi^i}{\partial x}(1+M^2\mathrm{Cos}^2(\alpha_1)) + \frac{\partial N_k^i}{\partial y} \quad \frac{\partial\psi^i}{\partial y}\left(1+M^2\mathrm{Sin}^2(\alpha_1) + \frac{\partial N_k^i}{\partial x} \quad \frac{\partial\psi^i}{\partial y}(1+M^2\mathrm{Sin}(2\alpha_1))\right)\right) \\ +\mathrm{Ra}\left(\theta^i\frac{\partial N_k^i}{\partial x} + \varphi^i\frac{\partial N_k^i}{\partial x}\right) \end{array} \right) d\Omega$$

$$= \int_\Gamma N_k^i\left(\frac{\partial\psi^i}{\partial x}\ n_x + \frac{\partial\psi^i}{\partial y}n_y\right)d\Gamma_i + \int_\Gamma N_k^i n_x\theta^i d\Gamma_i \quad (30)$$

Using (16) and (17) in (30) we have

$$\sum_m \psi_m^i \left\{ \int_\Omega \left(\begin{array}{l} \left(\frac{\partial N_k^i}{\partial x} \quad \frac{\partial N_m^i}{\partial x}(1+M^2\mathrm{Cos}^2(\alpha_1)) + \frac{\partial N_m^i}{\partial y} \quad \frac{\partial N_k^i}{\partial y}(1+M^2\mathrm{Sin}^2(\alpha_1)) + \right. \\ \left. + \frac{\partial N_k^i}{\partial x} \quad \frac{\partial N_m^i}{\partial y}(1+M^2\mathrm{Sin}(2\alpha_1)) + \right. \\ \left. + \mathrm{Ra}\sum_L(\theta_L^i\int_{\Omega\,i}\mathrm{N_k^i}\frac{\partial N_L^i}{\partial x} + \varphi_L^i N\int_{\Omega\,i}\mathrm{N_k^i}\frac{\partial N_L^i}{\partial x}d\Omega \right. \end{array} \right) d\Omega + \right\}$$

$$= \int_\Gamma N_k^i\left(\frac{\partial\psi^i}{\partial x}\ n_x + \frac{\partial\psi^i}{\partial y}n_y\right)d\Gamma_i + \int_\Gamma N_k^i\theta^i d\Omega_i = \Gamma_k^i \quad (31)$$

In this problem, we partitioned the region into uniform mesh of 9 triangular elements (Fig. 3.2) with global coordinates are (0, 0), (1, 0) and (1, h). Let e_1, e_2…..e_9 be the nine elements, let θ_1, θ_2, ….., θ_{10} be the global values of θ ,$\phi_1,\phi_2,\ldots\ldots,\phi_{10}$ be the global values of ϕ,and ψ_1, ψ_2,……ψ_{10} be the global values of ψ at the ten global nodes of the domain (Fig.2).

3.2 Shape Functions and Numerical Calculations

Range functions in $n_{i,j}$; *i* = element, *j* = node.

$$n_{1,2} = 3x - \frac{3y}{h},\quad n_{2,1} = 1 - \frac{3y}{h},\ n_{2,2} = -1 + \frac{3y}{h},\ n_{2,3} = 1 - 3x + \frac{3y}{h}$$

$$n_{3,1} = 2 - 3x,\quad n_{3,2} = -1 + 3x - \frac{3y}{h},\ n_{3,3} = \frac{3y}{h},$$

$$n_{4,1} = 1 - \frac{3y}{h},\ n_{4,2} = -2 + 3x,\quad n_{4,3} = 2 - 3x + \frac{3y}{h}$$

$$n_{5,1} = 2 - 3x,\quad n_{5,2} = -1 + 3x - \frac{3y}{h},\ n_{5,3} = \frac{3y}{h},$$

$$n_{6,1} = 2 - 3x\ ,\ n_{6,2} = 3x - \frac{3y}{h},\ n_{6,3} = 1 + \frac{3y}{h}$$

$$\underset{7,1}{n} = 2 - \frac{3y}{h},\ \underset{7,2}{n} = -2 + 3x,\ \underset{7,3}{n} = 1 - 3x + \frac{3y}{h}$$

$$\underset{8,1}{n} = 3 - 3x,\ \underset{8,2}{n} = -1 + 3x - \frac{3y}{h},$$

$$\underset{9,1}{n} = 2 - 3x,\ \underset{9,2}{n} = 3x - \frac{3y}{h},\quad \underset{9,3}{n} = -1 + \frac{3y}{h}$$

Substituting the above shape functions in (3.78), (3.79) & (3.74) w.r.to each element and integrating over the respective triangular domain we obtain the element in the form (25). The stiffness matrices are combined by inter element continuity conditions to get a 10x10 matrix equation for the global nodes ψ_p,θ_p and ϕ_p.

The global matrix equation for temperature (θ) is

$$A_3 X_3 = B_3 \tag{32}$$

The global matrix equation for concentration (ϕ) is

$$A_4 X_4 = B_4 \tag{33}$$

The global matrix equation for stream function (ψ) is

$$A_5 X_5 = B_5 \tag{34}$$

where

$$A_3 = \begin{bmatrix} -1 & a_{1,2} & a_{1,3} & 0 & 0 & 0 & 0 & 0 & 0 & 0 \\ 0 & a_{2,2} & a_{2,3} & 0 & 0 & 0 & 0 & 0 & 0 & 0 \\ 0 & a_{3,2} & a_{3,3} & a_{3,4} & a_{3,5} & 0 & 0 & 0 & 0 & 0 \\ 0 & 0 & a_{4,3} & a_{4,4} & a_{4,5} & 0 & 0 & 0 & 0 & 0 \\ 0 & 0 & a_{5,3} & a_{5,4} & a_{5,5} & a_{5,6} & a_{5,7} & 0 & 0 & 0 \\ 0 & 0 & 0 & 0 & a_{6,5} & a_{6,6} & a_{6,7} & 0 & 0 & 0 \\ 0 & 0 & 0 & 0 & a_{7,5} & a_{7,6} & a_{7,7} & a_{7,8} & a_{7,9} & 0 \\ 0 & 0 & 0 & 0 & 0 & 0 & a_{8,7} & a_{8,8} & a_{8,9} & 0 \\ 0 & 0 & 0 & 0 & 0 & 0 & a_{9,7} & a_{9,8} & a_{9,9} & 0 \\ 0 & 0 & 0 & 0 & 0 & 0 & 0 & 0 & a_{10,9} & a_{10,10} \end{bmatrix}$$

$$A_4 = \begin{bmatrix} 1 & b_{1,2} & b_{1,3} & 0 & 0 & 0 & 0 & 0 & 0 & 0 \\ 0 & b_{2,2} & b_{2,3} & 0 & 0 & 0 & 0 & 0 & 0 & 0 \\ 0 & b_{3,2} & b_{3,3} & b_{3,4} & b_{3,5} & 0 & 0 & 0 & 0 & 0 \\ 0 & 0 & b_{4,3} & b_{4,4} & b_{4,5} & 0 & 0 & 0 & 0 & 0 \\ 0 & 0 & b_{5,3} & b_{5,4} & b_{5,5} & b_{5,6} & b_{5,7} & 0 & 0 & 0 \\ 0 & 0 & 0 & 0 & b_{6,5} & b_{6,6} & b_{6,7} & 0 & 0 & 0 \\ 0 & 0 & 0 & 0 & b_{7,5} & b_{7,6} & b_{7,7} & b_{7,8} & b_{7,9} & 0 \\ 0 & 0 & 0 & 0 & 0 & 0 & b_{8,7} & b_{8,8} & b_{8,9} & 0 \\ 0 & 0 & 0 & 0 & 0 & 0 & b_{9,7} & b_{9,8} & b_{9,9} & 0 \\ 0 & 0 & 0 & 0 & 0 & 0 & 0 & 0 & b_{10,9} & b_{10,10} \end{bmatrix}$$

$$A_5 = \begin{bmatrix} 1 & a_{1,2} & a_{1,3} & 0 & 0 & 0 & 0 & 0 & 0 & 0 \\ 0 & a_{2,2} & a_{2,3} & 0 & 0 & 0 & 0 & 0 & 0 & 0 \\ 0 & a_{3,2} & a_{3,3} & a_{3,4} & a_{3,5} & 0 & 0 & 0 & 0 & 0 \\ 0 & 0 & a_{4,3} & a_{4,4} & a_{4,5} & 0 & 0 & 0 & 0 & 0 \\ 0 & 0 & a_{5,3} & a_{5,4} & a_{5,5} & a_{5,6} & a_{5,7} & 0 & 0 & 0 \\ 0 & 0 & 0 & 0 & a_{6,5} & a_{6,6} & a_{6,7} & 0 & 0 & 0 \\ 0 & 0 & 0 & 0 & a_{7,5} & a_{7,6} & a_{7,7} & a_{7,8} & a_{7,9} & 0 \\ 0 & 0 & 0 & 0 & 0 & 0 & a_{8,7} & a_{8,8} & a_{8,9} & 0 \\ 0 & 0 & 0 & 0 & 0 & 0 & a_{9,7} & a_{9,8} & a_{9,9} & 0 \\ 0 & 0 & 0 & 0 & 0 & 0 & 0 & 0 & a_{10,9} & a_{10,10} \end{bmatrix}, X_3 = \begin{pmatrix} \theta_1 \\ \theta_2 \\ \theta_3 \\ \theta_4 \\ \theta_5 \\ \theta_6 \\ \theta_7 \\ \theta_8 \\ \theta_9 \\ \theta_{10} \end{pmatrix}$$

$$X_4 = \begin{pmatrix} \phi_1 \\ \phi_2 \\ \phi_3 \\ \phi_4 \\ \phi_5 \\ \phi_6 \\ \phi_7 \\ \phi_8 \\ \phi_9 \\ \phi_{10} \end{pmatrix}, X_5 = \begin{pmatrix} \psi_1 \\ \psi_2 \\ \psi_3 \\ \psi_4 \\ \psi_5 \\ \psi_6 \\ \psi_7 \\ \psi_8 \\ \psi_9 \\ \psi_{10} \end{pmatrix}, B_3 = \begin{pmatrix} ar_1 \\ ar_2 \\ ar_3 \\ ar_4 \\ ar_5 \\ ar_6 \\ ar_7 \\ ar_8 \\ ar_9 \\ ar_{10} \end{pmatrix}, B_4 = \begin{pmatrix} br_1 \\ br_2 \\ br_3 \\ br_4 \\ br_5 \\ br_6 \\ br_7 \\ br_8 \\ br_9 \\ br_{10} \end{pmatrix}, B_5 = \begin{pmatrix} cr_1 \\ cr_2 \\ cr_3 \\ cr_4 \\ cr_5 \\ cr_6 \\ cr_7 \\ cr_8 \\ cr_9 \\ cr_{10} \end{pmatrix}$$

where ar_1, ar_2,…..ar_{10}, br_1, br_2, …..br_{10}, cr_1, cr_2, …cr_{10}, $a_{1,2}$, $a_{1,3}$,…$a_{10,10}$, $b_{1,2}$, $b_{1,3}$,…$b_{10,10}$ are constants involving parameters.

In view of the condition (14) and (15) on the boundary the specified boundary conditions as the primary variable ψ are ψ = 0 on the boundary of the duct. Likewise the boundary conditions on the θ and C at the side wall gives

$$\theta_4 = \theta_5 = \theta_9 = \theta_{10} = 1$$
$$C_4 = C_5 = C_9 = C_{10} = 1 \quad (35)$$

Initially we choose ψ as zero and solve the equations (32) and (33) we get first approximation values of θ andϕ. Now using these θ_i and ϕ_i in (34) we get ψ_i. Now in the second iteration, by putting these ψ_i values in (32) and (33) we get second approximation values of θ, ϕ and vice versa. The matrix equations are assembled to get global matrix equation for the whole domain, which is then solved iteratively, to obtain θ, ψ and ϕ in porous medium. In order to get accurate results, tolerance level of solution for θ, ψ and ϕ are set at 10^{-5}, 10^{-5} and 10^{-9} respectively. Element size in domain varies. Large number of elements are located near the walls where large variations in θ, ψ and ϕ are expected. The mesh is symmetrical about central horizontal and vertical lines of the cavity. Sufficiently dense mesh is chosen to make the solution mesh invariant. The mesh size of 3200 elements has good accuracy in predicting the heat transfer behavior of the porous medium. The computations are carried out on high-end computer.

On the boundary wall x=1, the Nusselt number and Sherwood number are calculated using the formula.

$$\text{Nu} = \left(\frac{\partial \theta}{\partial x}\right)_{x=1 \text{ and }} \text{Sh} = \left(\frac{\partial \varphi}{\partial x}\right)_{x=1}$$

Nusselt Number &Sherwood Number on the side wall x=1 for different regions are given by

$$Nu_1 = \left(n_{5,1}\right)_x \theta_3 + \left(n_{5,2}\right)_x \theta_4 + \left(n_{5,3}\right)_x \theta_5, Sh_1 = \left(n_{5,1}\right)_x \phi_3 + \left(n_{5,2}\right)_x \phi_4 + \left(n_{5,3}\right)_x \phi_5, (0 \le y \le h/3)$$

$$Nu_2 = \left(n_{6,1}\right)_x \theta_6 + \left(n_{6,2}\right)_x \theta_5 + \left(n_{6,3}\right)_x \theta_9, Sh_2 = \left(n_{6,1}\right)_x \phi_6 + \left(n_{6,2}\right)_x \phi_5 + \left(n_{6,3}\right)_x \phi_9 \; h/3 \le y \le 2h/3)$$

$$Nu_3 = \left(n_{9,1}\right)_x \theta_8 + \left(n_{9,2}\right)_x \theta_9 + \left(n_{9,3}\right)_x \theta_{10}, Sh_3 = \left(n_{9,1}\right)_x \phi_8 + \left(n_{9,2}\right)_x \phi_9 + \left(n_{9,3}\right)_x \phi_{10} \quad (2h/3 \le y \le h) \quad (36)$$

The suffix 'x' denotes differentiation of the shape functions with respect to 'x'.

Substituting the shape functions and the boundary conditions (35) in (36) the Nusselt Number and the Sherwood Number in different regions are

Nu_1=3-3θ_3, Sh_1=3-3ϕ_3 $\left(0 \le y \le h/3\right)$,

Nu_2=3-3θ_6, Sh_2=3-3ϕ_6 $\left(h/3 \le y \le 2h/3\right)$

Nu_3=3-3θ_8, Sh_3=3-3ϕ_8 $\left(2h/3 \le y \le h\right)$

3.3. Comparison:

Comparing the present results with the results of Shanti *et al*.[40] without inclined magnetic field ($\alpha_1 = 0$) and chemical reaction effects (γ=0). In the absence of mass transfer and chemical reaction the results coincide with Badruddin *et al.* [34].

Table-1: Values of Nusselt number and Sherwood number on the wall x=1 when α_1=0andγ=0 with N and Sr.

N	1	2	-0.5	-0.8	1	1	1
Sr	0.5	0.5	0.5	0.5	1.0	1.5	2
Nu_1	61.1299	52.4987	10.1099	9.8589	61.9989	64.1089	66.1399
Nu_2	58.1711	51.0387	11.1266	9.8299	59.1078	60.1809	61.7899
Nu_3	54.3895	50.1999	11.7678	9.8398	55.1066	56.2706	57.3798
Sh_1	21.9423	20.6099	3.3549	4.1489	15.4027	13.1099	11.8897
Sh_2	26.5145	21.1298	4.6935	5.1889	11.1709	19.0599	18.8099
Sh_3	19.1128	29.6991	60.1087	6.2309	18.1599	17.0899	16.1289

Table-2: Results obtained by Shanti et al. [40] with N and Sr.

N	1	2	-0.5	-0.8	1	1	1
Sr	0.5	0.5	0.5	0.5	1.0	1.5	2
Nu_1	61.1251	52.523	10.214	9.867	62.524	64.129	66.134
Nu_2	58.161	51.135	11.165	9.856	59.126	60.196	61.896
Nu_3	54.492	50.202	11.793	9.854	55.098	56.289	57.381
Sh_1	21.944	20.430	3.3792	4.135	15.425	13.126	11.896
Sh_2	26.516	21.116	4.6930	51.792	11.169	19.056	18.809
Sh_3	19.092	29.70	6.0072	6.231	18.176	17.069	16.124

4. RESULTSAND DISCUSSIONS

The aim of this analysis is to investigate the effect of dissipation, thermo-diffusion and thermal radiation on the convective heat and mass transfer flow of a viscous chemically reacting electrical conducting fluid through a porous medium in a rectangular duct under the action of an inclined magnetic field.

The actual temperature (θ) is exhibited in figures 3-22 for different values of Sr, Ec, N_1, γ and α_1 at different horizontal and vertical levels. Figs.3-6 depicts θ with radiation parameter N_1. It is observed from these figures greater the radiative heat flux smaller the actual temperature at x=2/3 level while at y=h/3,y=2h/3 and x=1/3 levels it enhances with N_1. Figs.7-10 represent θ with Eckert number Ec. The actual temperature depreciates with increase in Ec at all levels. Figs.11-14 depict the temperature with thermo-diffusion effect (Sr). It is noticed that that the actual temperature diminishes at x=1/3 and strengthens at y = 2h/3 level and (figs.11& 13) while at x=2/3 & y=h/3, the actual temperature diminishes with rise in Sr≤1.0 and strengthens Sr>1.5 and |Sr|<0 (figs.12 & 14). The effect of chemical reaction on temperature at different levels is shown in figs.15-18. We noticed that the actual temperature increases at y=h/3 & x=1/3 levels in both degenerating and generating chemical reaction (fig 16 &17). The actual temperature reduces at x=2/3 level and y=2h/3 level (figs.15&18). The influence of inclined magnetic field on θ is shown in figs.19-22 at different levels. Rise in the inclination α_1 enhances the actual temperature at y=2h/3 level (fig.19) and depreciates at all vertical levels and at horizontal level y=h/3(fig 20-23).

The concentration distribution (ϕ) is shown in figs.24-43 for different parametric values. We follow the convention that the concentration is positive or negative according as the actual concentration C is greater or lesser than C_c, the concentration on the cold wall. Figs.24-27 represent the variation of the concentration with radiation parameter N_1 .We noticed that greater the radiative heat flux smaller the actual concentration at y=2h/3, x=1/3 and x=2/3 figs (24, 26&27) while larger the actual concentration at y=h/3(fig.25). The effect of dissipation on the concentration is shown at different levels in figs.28-31. It can be seen from the profiles that higher the dissipative heat smaller the actual concentration at all vertical levels and at horizontal level y=2h/3 level (fig 28, 30 & 31).At y=h/3 level it enhances in the vertical strip (fig29).

Figs. 32-35 represent the effect of thermo-diffusion on ϕ. We noticed from the profiles that the actual concentration diminishes with Sr <1 and strengthens with higher Sr>1.5 at y=h/3 and x=1/3 levels. Also it reduces with |Sr|(<0)(figs.33-34) .At x=2/3 level the actual concentration reduces in the horizontal strip (0≤y≤0.33) and enhances in the region (0.33≤y≤0.66) with Sr<1.0.For higher Sr>1.5 and |Sr|(<0) we notice an enhancement in the horizontal strip(0,0.33) and reduces in the region (0.33,0.66) (fig 35). At y=2h/3 level it strengthens with Sr<1 and reduces with Sr>1.5 also it reduces at |Sr|(<0) (fig.32). The effect of chemical reaction on ϕ is exhibited in figs36-39 at different levels. We noticed that the actual concentration diminishes for γ>0 and enhances in the γ<0 at all horizontal and vertical level x=2/3 level (figs.36, 37& 39).At x=1/3 it reduces in both the cases (fig 38). The influence of inclination of the magnetic field (α_1) on ϕ is shown in figs.40-43 at different levels. We noticed that rise in $\alpha_1 \leq \pi/2$ goes to a depreciation in the actual concentration and enhances with higher $\alpha_1 \geq \pi$ at y=2h/3(fig40). At x=2/3&y=h/3 levels the actual concentration enhances and reduces at x=1/3 level (fig42) with increase in α_1 (figs. 41 & 43).

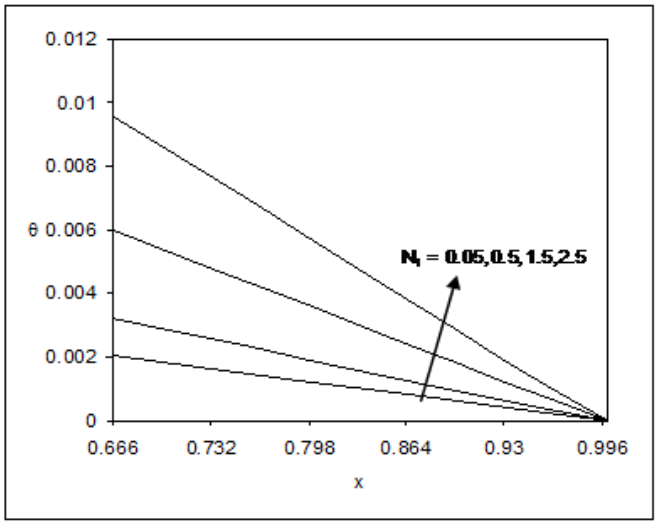

Fig.3: Variation of Temperature (θ) with Thermal radiation (N_1) at $y = \frac{2h}{3}$ level.

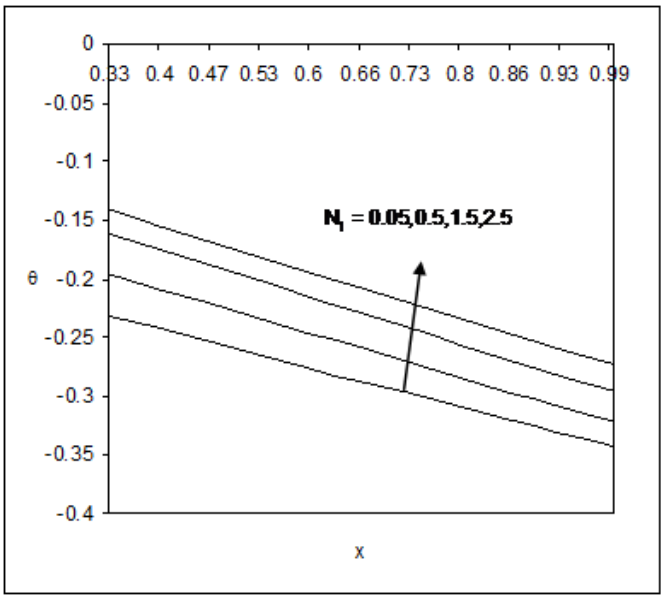

Fig.4: Temperature (θ) with Thermal Radiation (N_1) at $y = \frac{h}{3}$ level.

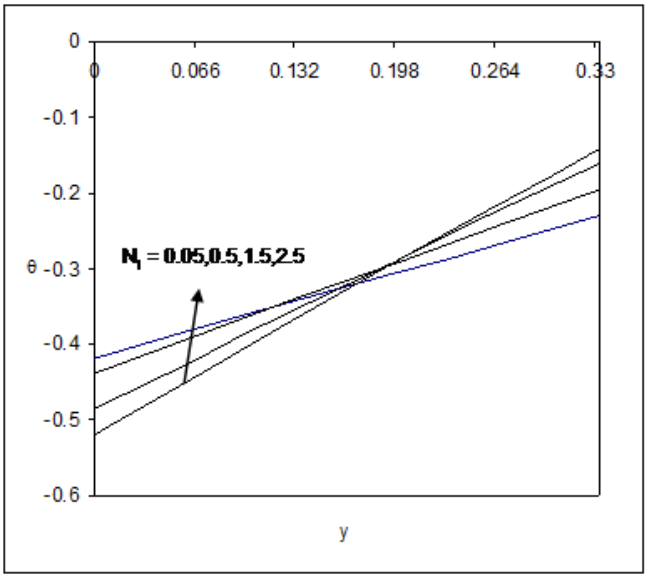

Fig.5: Temperature (θ) with Thermal Radiation (N_1) at $x = \frac{1}{3}$ level.

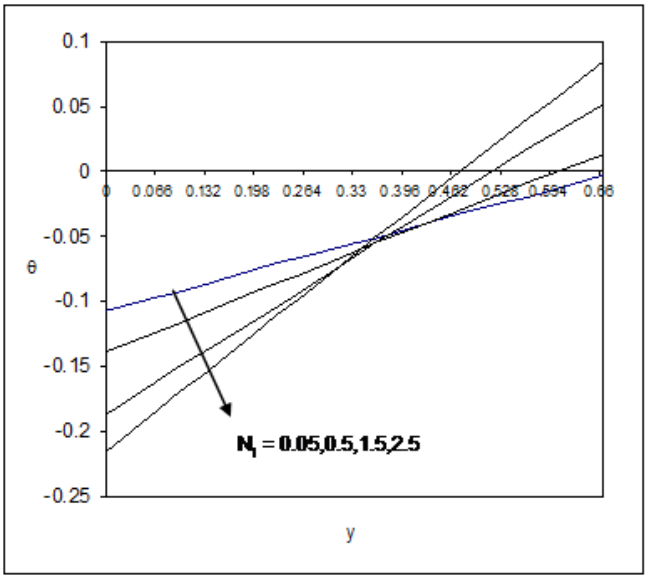

Fig.6: Temperature (θ) with Thermal Radiation (N_1) at $x = \frac{2}{3}$ level.

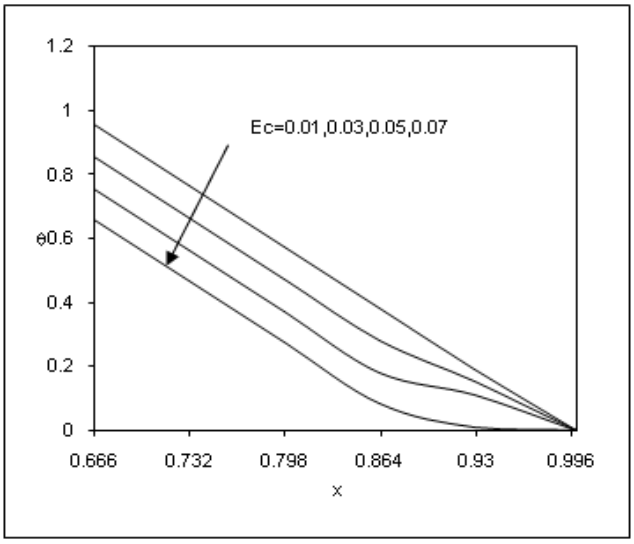

Fig.7: Temperature (θ) with Eckert Number (Ec) at $y = \frac{2h}{3}$ level.

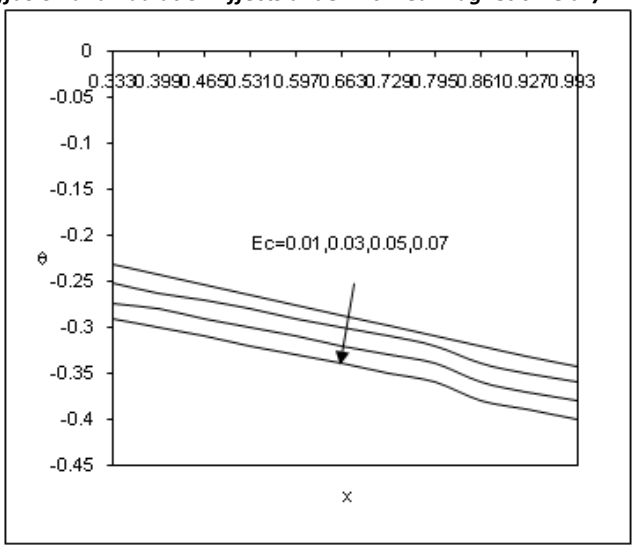

Fig.8: Temperature (θ) with Eckert Number (Ec) at $y = \frac{h}{3}$ level.

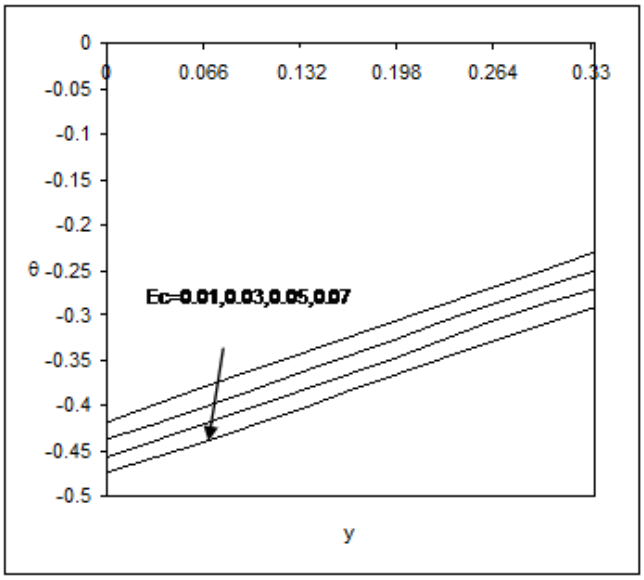

Fig.9: Temperature (θ) with Eckert Number (Ec) at $x = \frac{1}{3}$ level.

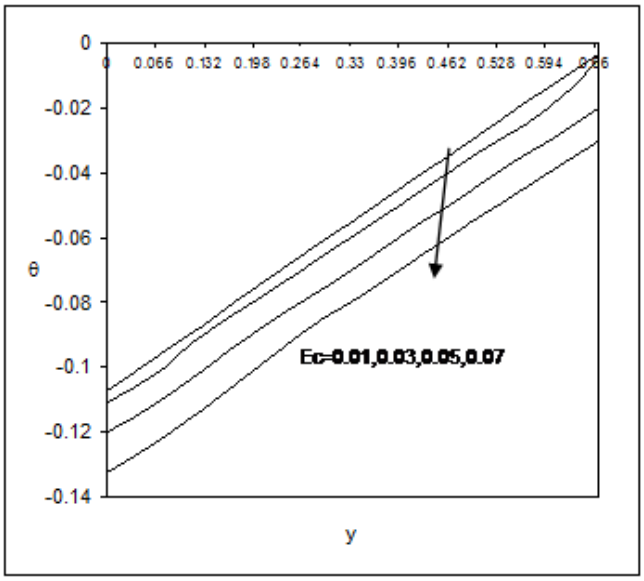

Fig.10: Temperature (θ) with Eckert number (Ec) at $x = \frac{2}{3}$ level.

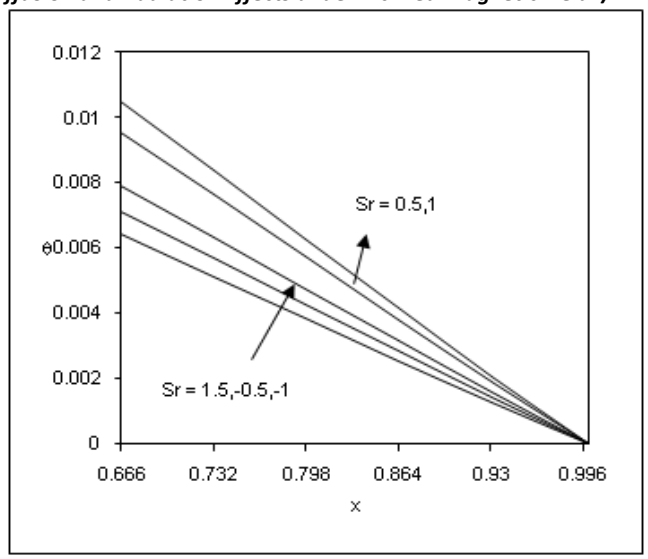

Fig. 11: Temperature (θ) with Soret Parameter (Sr) at $y = \frac{2h}{3}$ level.

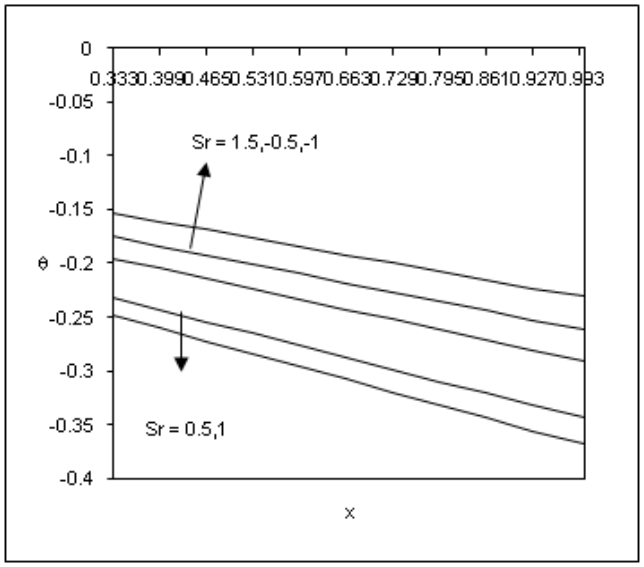

Fig. 12: Temperature (θ) with Soret Parameter (Sr) at $y = \frac{h}{3}$ level.

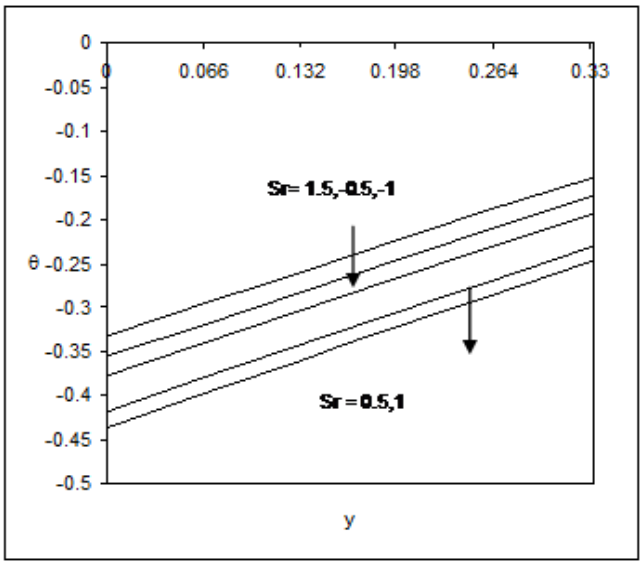

Fig.13: Temperature (θ) with Soret parameter (Sr) at $x = \frac{1}{3}$ level.

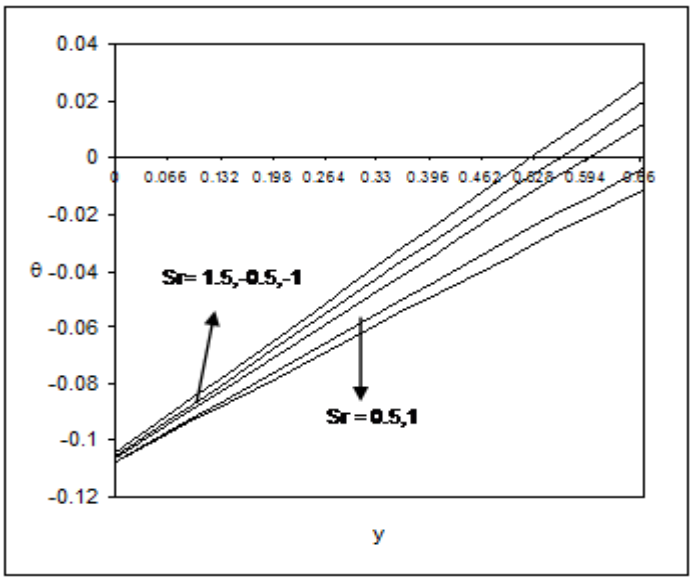

Fig. 14: Temperature (θ) with Soret Parameter (Sr) at $x = \frac{2}{3}$ level.

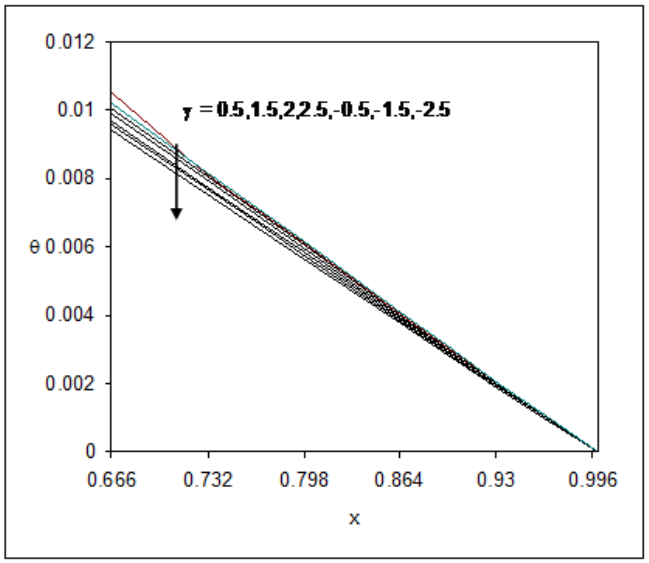

Fig. 15: Temperature (θ) with Chemical reaction parameter (γ) at $y = \frac{2h}{3}$ level.

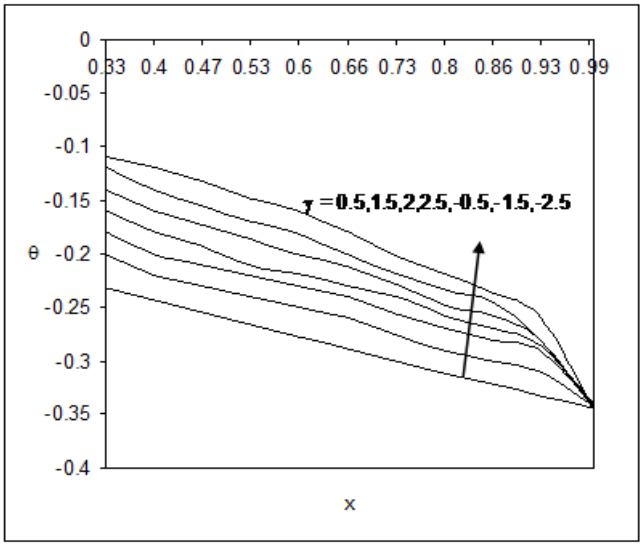

Fig. 16: Temperature (θ) with Chemical reaction parameter (γ) at $y = \frac{h}{3}$ level.

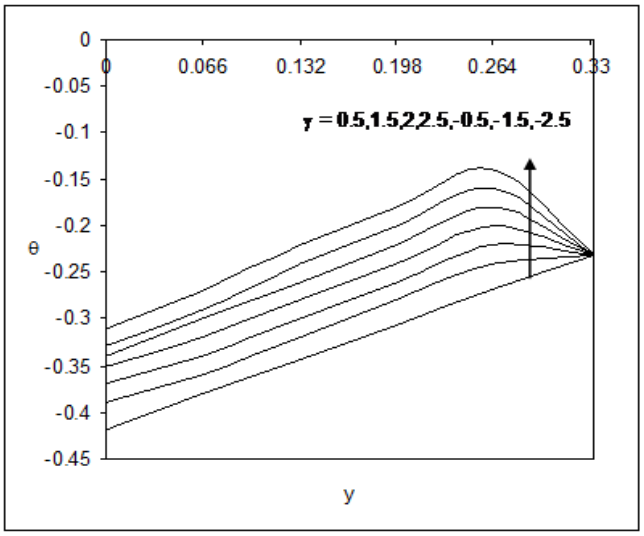

Fig. 17: Temperature (θ) with Chemical reaction parameter (γ) at $x = \frac{1}{3}$ level.

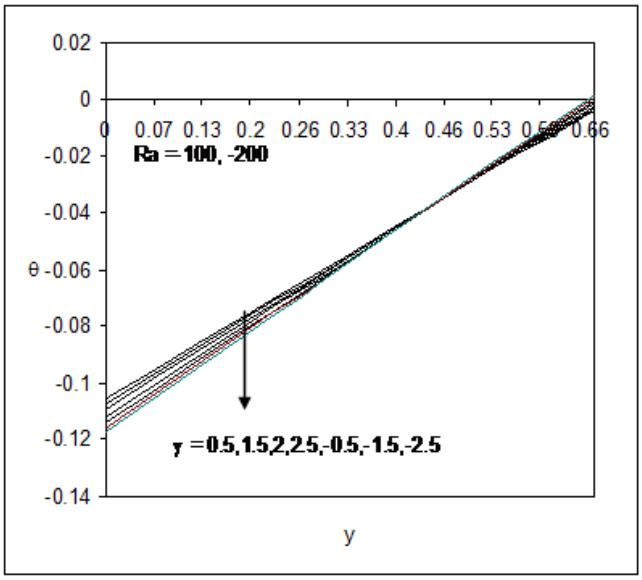

Fig. 18: Temperature (θ) with Chemical reaction parameter (γ) at $x = \frac{2}{3}$ level.

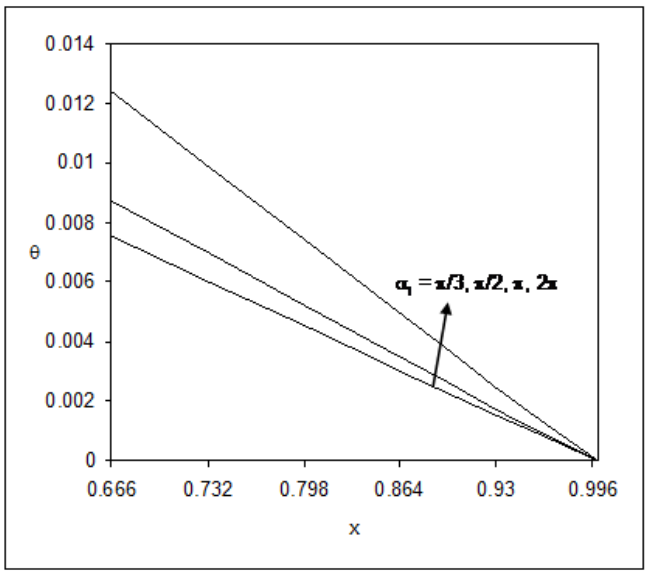

Fig.19: Temperature (θ) with angle of inclination (α_1) at $y = \frac{2h}{3}$ level.

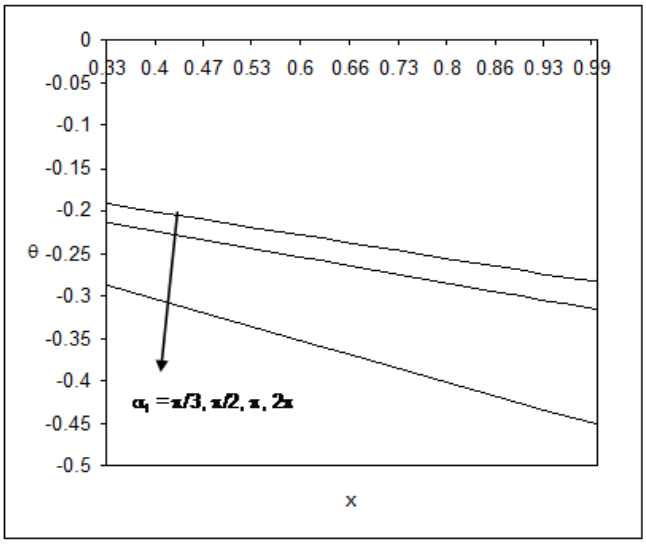

Fig.20: Temperature (θ) with angle of inclination (α_1) at $y = \frac{h}{3}$ level.

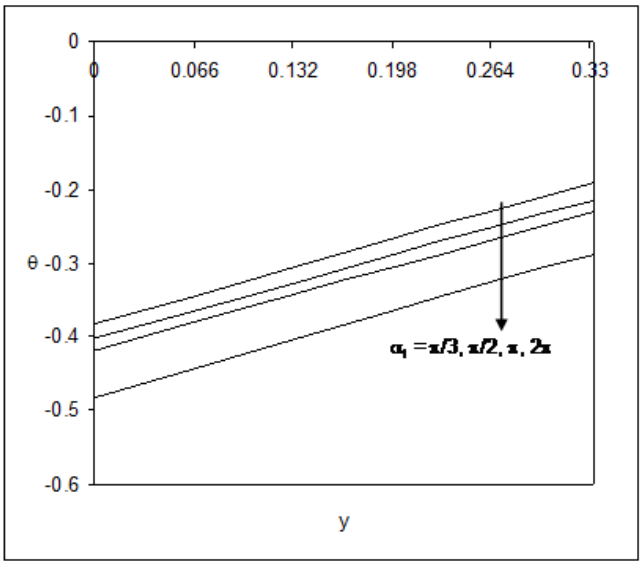

Fig. 21: Temperature (θ) with angle of inclination (α_1) at $x = \frac{1}{3}$ level.

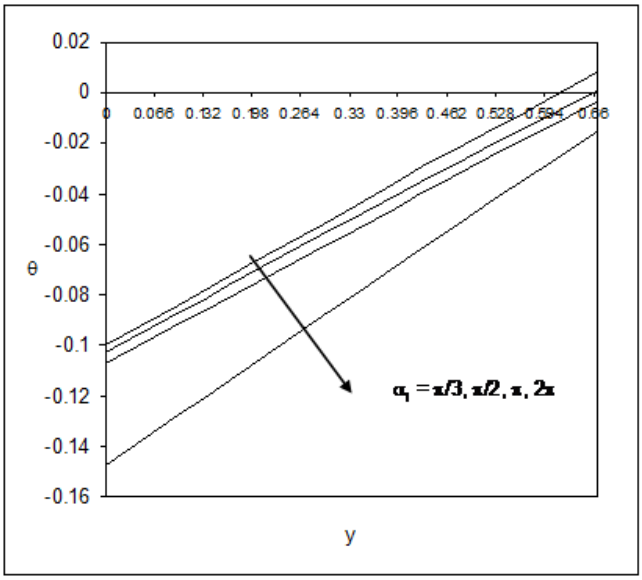

Fig. 22: Temperature (θ) with angle of inclination (α_1) at $x = \frac{2}{3}$ level.

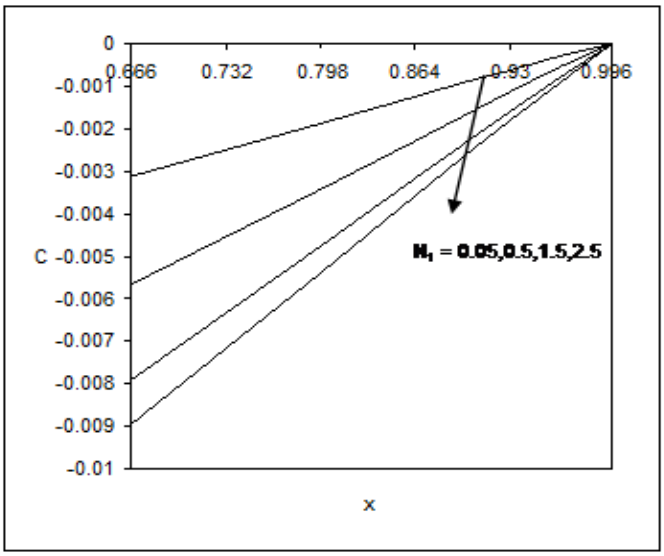

Fig. 23: Variation of concentration (ϕ) with Thermal radiation (N_1) at $y = \frac{2h}{3}$ level.

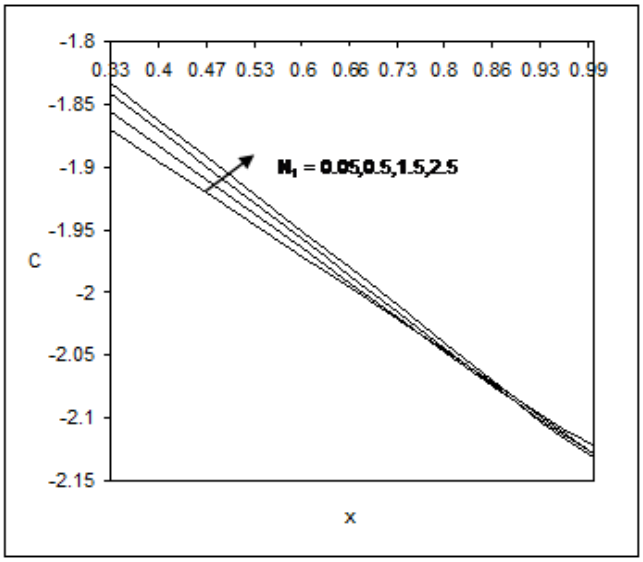

Fig. 24: Concentration (ϕ) with Thermal radiation (N_1) at $y = \frac{h}{3}$ level.

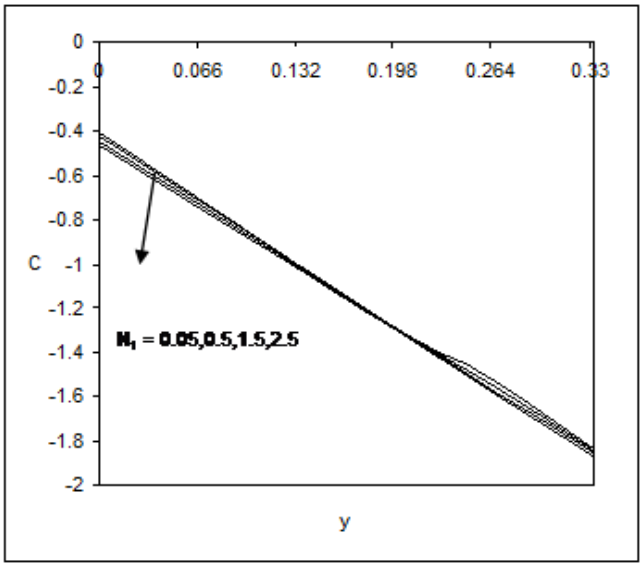

Fig.25: Concentration (ϕ) with Thermal radiation (N_1) at $x = \frac{1}{3}$ level.

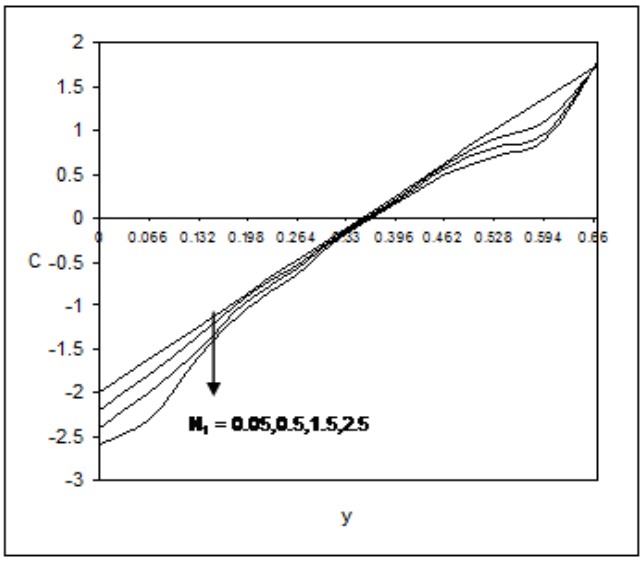

Fig.26: Concentration (ϕ) withThermal radiation (N_1) at $x = \frac{2}{3}$ level.

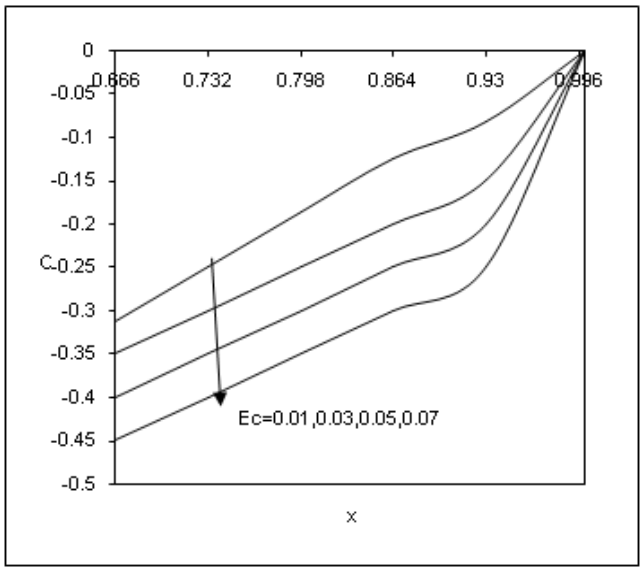

Fig.27: Concentration (ϕ) with Eckert number (Ec) at $y = \frac{2h}{3}$ level.

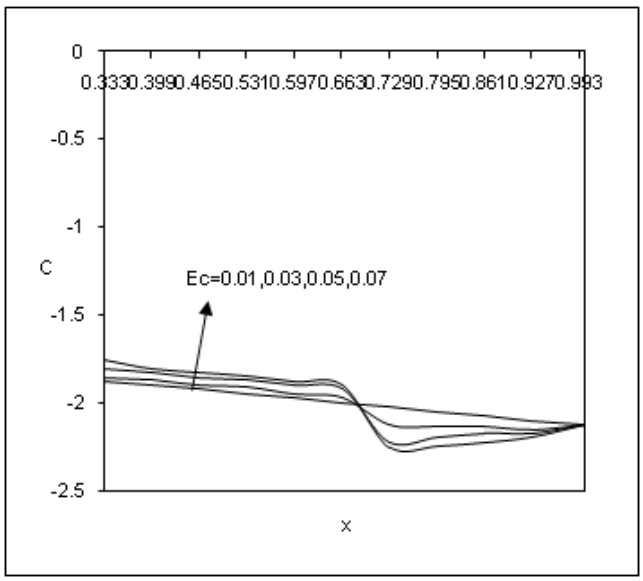

Fig.28: Concentration (ϕ) with Eckert number (Ec) at $y = \frac{h}{3}$ level.

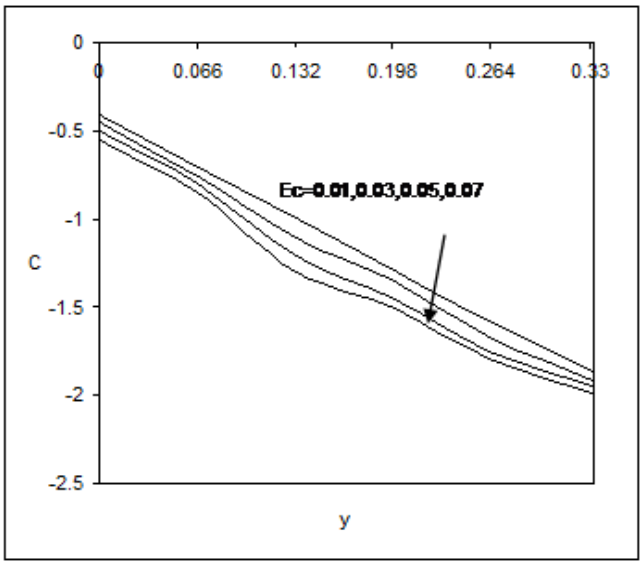

Fig.29: Concentration (ϕ) with Eckert number (Ec) at $x = \frac{1}{3}$ level.

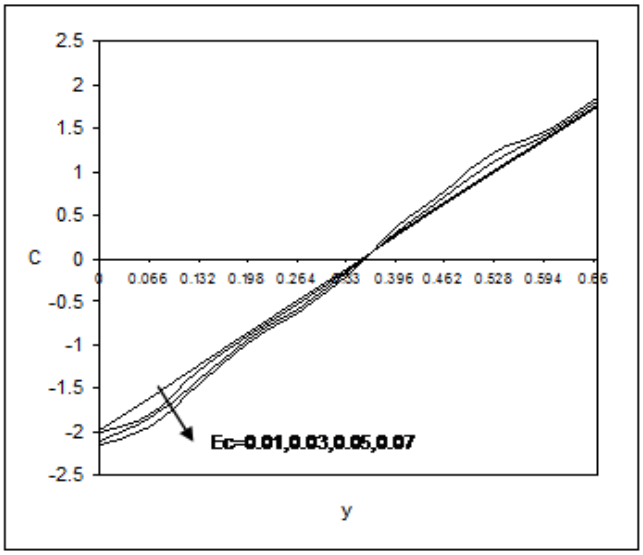

Fig.30: Concentration (ϕ) with Eckert number (Ec) at $x = \frac{2}{3}$ level.

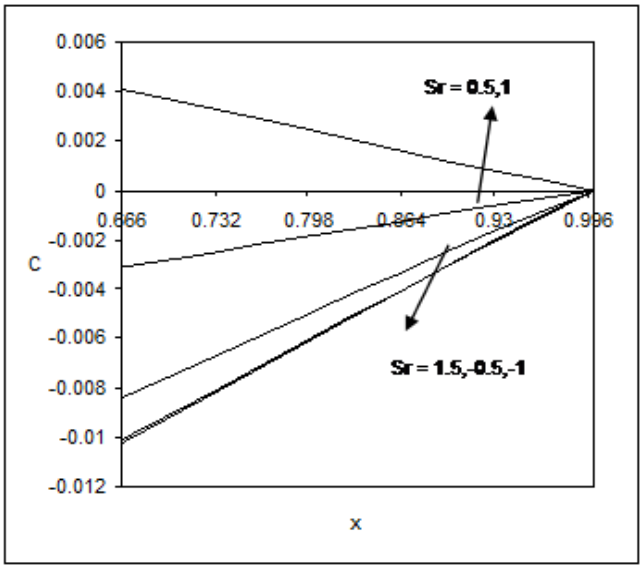

Fig.31: Concentration (ϕ) with Soret parameter (Sr) at $y = \frac{2h}{3}$ level.

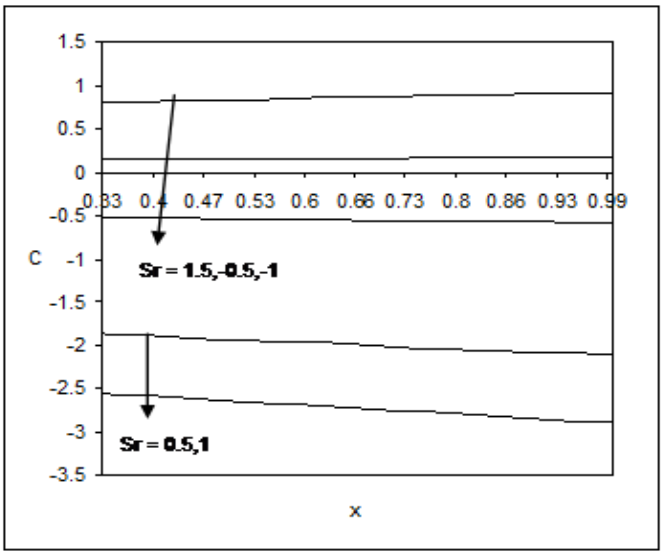

Fig.32: Concentration (ϕ) with Soret parameter (Sr) at $y = \frac{h}{3}$ level.

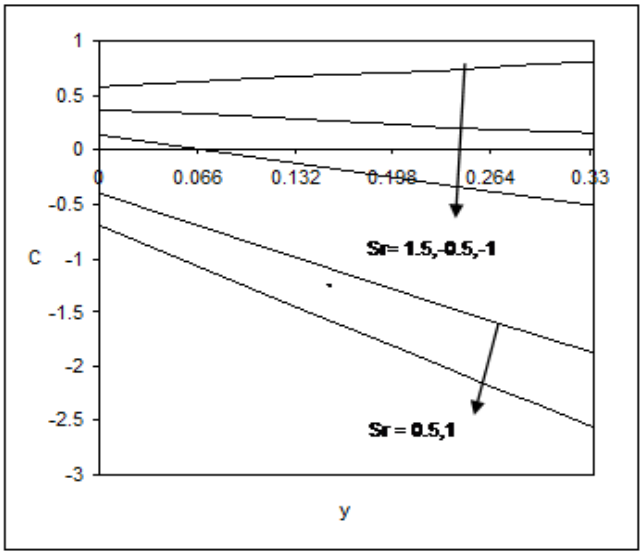

Fig.33: Concentration (ϕ) with Soret parameter (Sr) at $x = \frac{1}{3}$ level

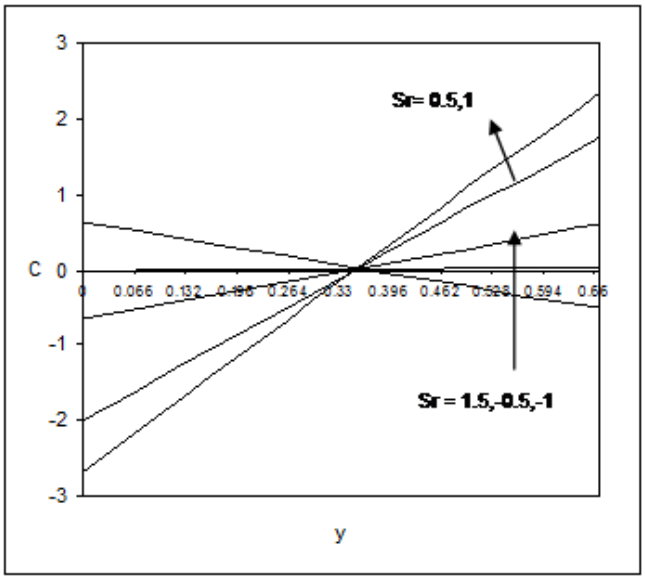

Fig.34: Concentration (ϕ) with soret parameter (Sr) at $x = \frac{2}{3}$ level.

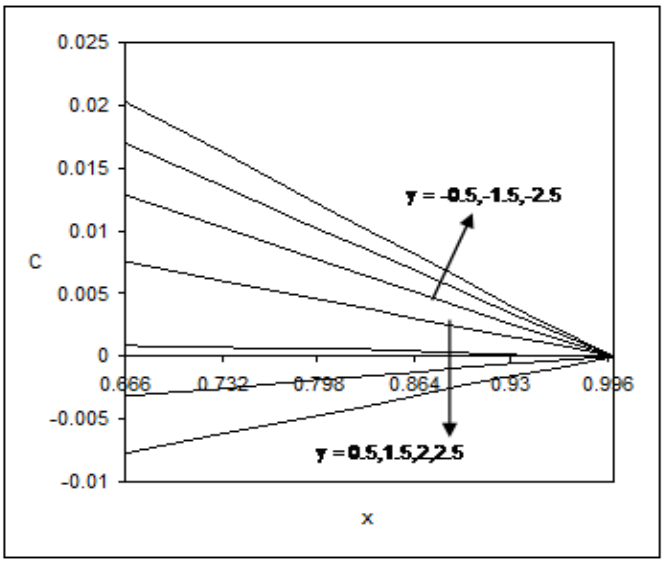

Fig. 35: Concentration (ϕ) with chemical reaction parameter (γ) at $y = \frac{2h}{3}$ level.

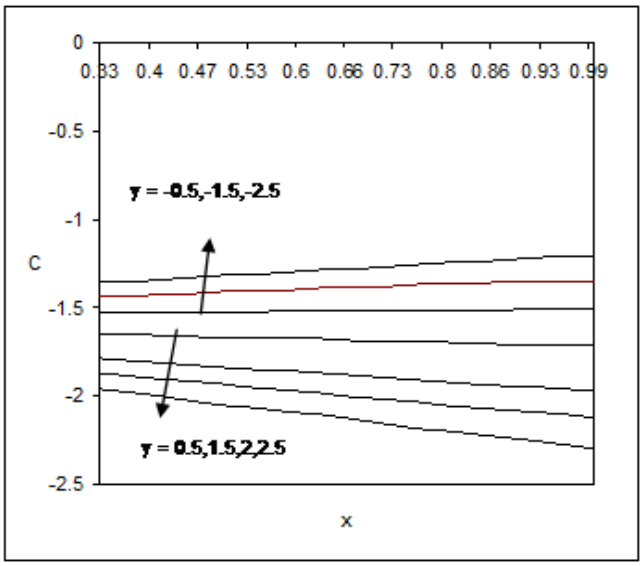

Fig.36: Concentration (ϕ) with chemical reaction parameter (γ) at $y = \frac{h}{3}$ level.

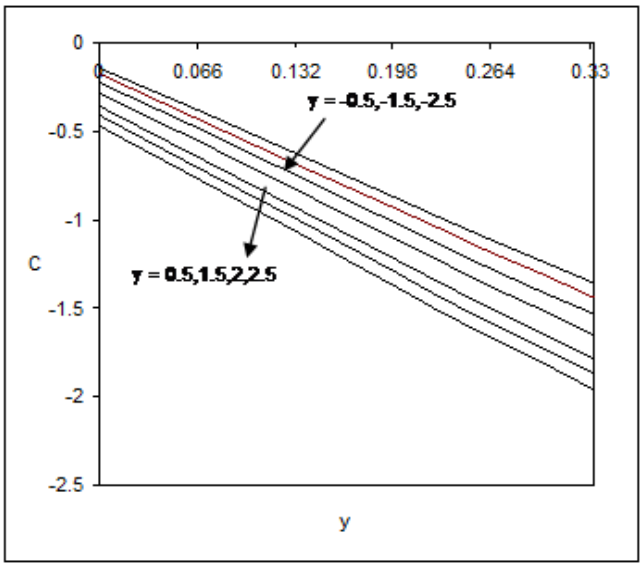

Fig.37: Concentration (ϕ) with chemical reaction parameter (γ) at $x = \frac{1}{3}$ level.

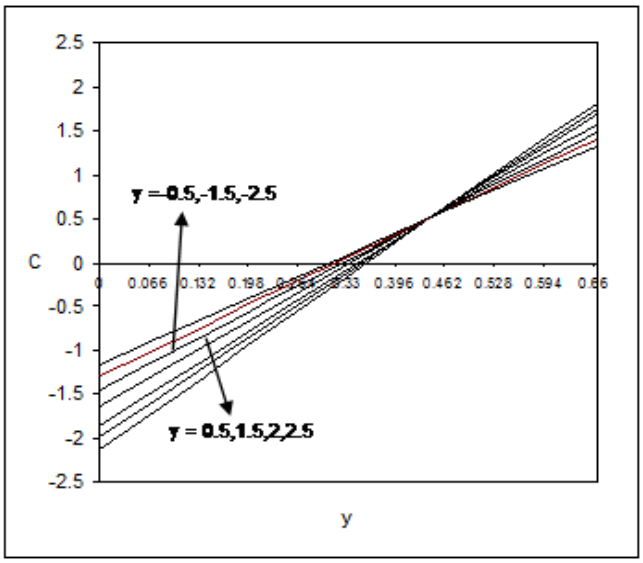

Fig.38: Concentration (ϕ) with chemical reaction parameter (γ) at $x = \frac{2}{3}$ level.

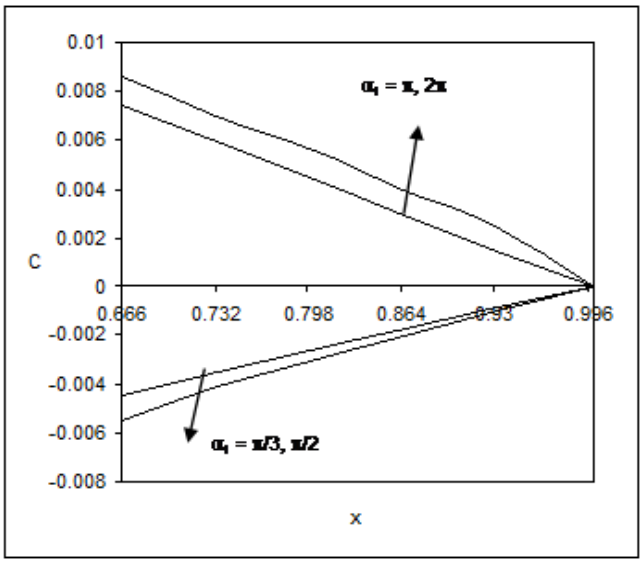

Fig.39: Concentration (ϕ) with angle of inclination (α_1) at $y = \frac{2h}{3}$ level.

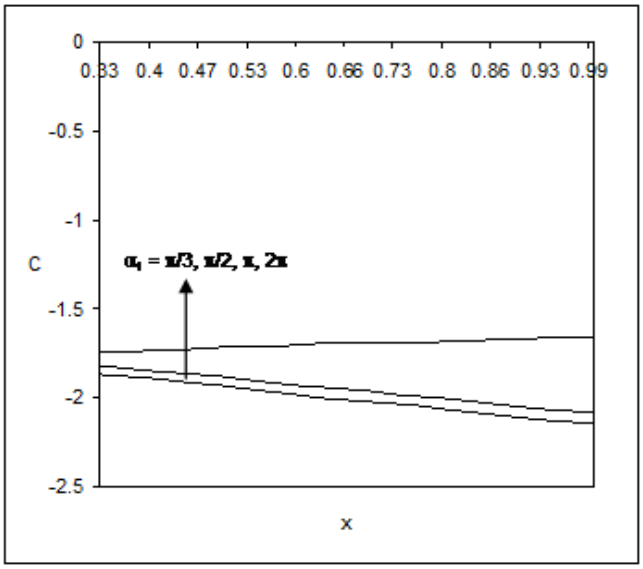

Fig.40: Concentration (ϕ) with angle of inclination (α_1) at $y = \frac{h}{3}$ level.

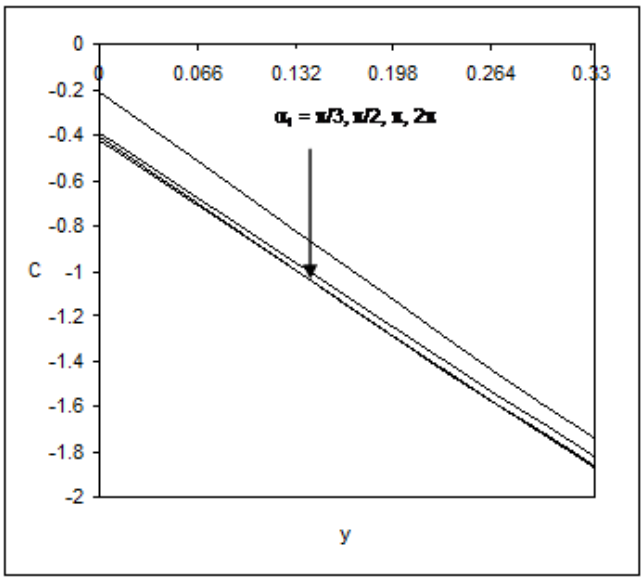

Fig.41: Concentration (ϕ) with angle of inclination (α_1) at $x = \frac{1}{3}$ level.

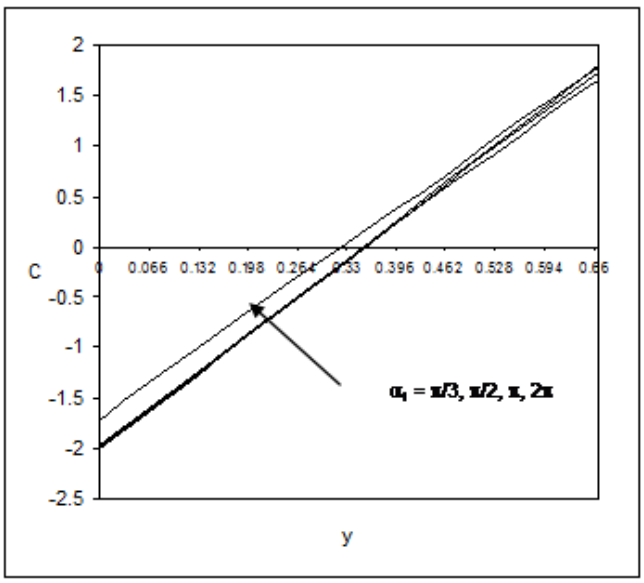

Fig.42: Concentration (ϕ) with angle of inclination (α_1) at $x = \frac{2}{3}$ level.

The rate of heat transfer (Nusselt number) on x=1 at different levels is exhibited in tables 3-4 for different parametric values. We noticed that the rate of heat transfer reduces as we move from bottom wall to the top wall of the rectangle. With respect to Soret parameter Sr, we find that the Nusselt number on first and intermediate quadrants enhances with Sr and reduces on the uppermost quadrant. With reference to the radiation parameter N_1 we find that an increase in N_1 enhances |Nu| on the lower and intermediate quadrants and diminishes on the uppermost quadrant with $N_1 \leq 1.5$ and higher $N_1 \geq 2.5$ enhances |Nu| on the lower quadrant and reduces on the middle and upper quadrants. The transition of Nu with Eckert number Ec shows that the rate of heat transfer reduces on the lower quadrant and enhances in the intermediate and upper quadrants with $Ec \leq 0.03$ and enhances on all the quadrants $Ec \geq 0.05$. According to the chemical reaction parameter γ, we find that an increase in $\gamma \leq 1.5$, enhances |Nu| on all three quadrants while for higher $\gamma \geq 2.5$, |Nu| reduces on the lower and intermediate quadrants and enhances on the uppermost quadrant. In the case of generating chemical reaction case, |Nu| reduces on all three quadrants with $|\gamma| \leq 1.5$ and enhances on the lower and intermediate quadrants and reduces on uppermost quadrant with higher $|\gamma| \geq 2.5$. The variation of inclination of the magnetic field on Nu shows that the Nusselt number on the three quadrants reduces with increase in $\alpha_1 \leq \pi$ and enhances with higher $\alpha_1 \geq 2\pi$ (table 4.8).

The rate of mass transfer (Sherwood Number) is exhibited in tables 5-6 for different parametric values. The rate of mass transfer enhances as we move along the line x=1. The variation of Sh with Soret parameter Sr indicates that |Sh| experiences an enhancement with Sr on all the quadrants. With reference to N_1, it is observed that the rate of mass transfer on all the three quadrants enhances with increase in N_1. With respect to Ec, we find that $|Sh_1|$ enhances with Ec, $|Sh_2|$ diminishes with Ec$\leq$ 0.03 and increases with greater Ec $\geq$ 0.05 while Sh_3 enhances with Ec$\leq$ 0.03 and reduces with Ec$\geq$ 0.04. The transition of Sh with chemical reaction parameter γ shows that the |Sh| on all the three quadrants reduces with $\gamma \leq 1.5$ and Sherwood number enhances with higher $\gamma \geq 2.5$. For $\gamma < 0$ an increase in $|\gamma|$ reduces |Sh| on all the three quadrants. An increase in the inclination $\alpha_1 \leq \pi/3$ enhances Sh and |Sh| reduces with higher $\alpha_1 \geq \pi$ on all the three quadrants.

	I	II	III	IV	V	VI	VII	VIII	IX	X
Nu1	2.4297	2.7461	2.8618	2.4296	2.4310	2.4363	2.4296	2.4682	2.4552	2.4625
Nu2	2.2219	2.2792	2.2232	2.2221	2.2224	2.2239	2.2219	2.2413	2.2293	2.2299
Nu3	2.0132	1.8932	1.6656	2.0144	2.0145	2.0142	2.0688	2.0039	2.0029	2.0016
N_1	**0.5**	**1.5**	**2.5**	**0.5**	**0.5**	**0.5**	**0.5**	**0.5**	**0.5**	**0.5**
Ec	**0.01**	**0.01**	**0.01**	**0.03**	**0.05**	**0.01**	**0.01**	**0.01**	**0.01**	**0.01**
γ	**0.5**	**0.5**	**0.5**	**0.5**	**0.5**	**1.5**	**2.5**	**-0.5**	**-1.5**	**-2.5**

Table-3: Nusselt Number(Nu) at x=1in different regions with N_1, Ec, γ.

	I	II	III	IV	V
Nu1	2.4297	2.4102	2.4004	2.5913	2.4289
Nu2	2.2219	2.2007	2.1841	2.3221	2.2376
Nu3	2.0132	1.9956	1.9682	2.0608	1.9557
α_1	**$\pi/4$**	**$\pi/3$**	**π**	**2π**	**$\pi/4$**
Sr	**0.5**	**0.5**	**0.5**	**0.5**	**1.5**

Table-4: Nusselt Number(Nu) at x=1in different regions with α_1, Sr.

	I	II	III	IV	V	VI	VII	VIII	IX	X
Sh1	9.9637	9.9638	11.9639	9.0379	10.7518	7.8009	7.1759	6.6668	10.1802	10.2531
Sh2	2.6029	2.5021	2.5032	2.3643	2.6613	6.9528	6.8071	1.6885	2.6038	2.6043
Sh3	-4.957	-5.157	-4.957	-4.609	-5.229	-3.571	-3.57	-3.288	-4.080	-4.060
Ec	**0.01**	**0.03**	**0.05**	**0.01**	**0.01**	**0.01**	**0.01**	**0.01**	**0.01**	0.01
γ	**0.5**	**0.5**	**0.5**	**1.5**	**2.5**	**-0.5**	**-1.5**	**-2.5**	**0.5**	**0.5**
N1	**0.5**	**0.5**	**0.5**	**0.5**	**0.5**	**0.5**	**0.5**	**0.5**	**1.5**	**2.5**

Table-5: Sherwood Number(Sh) at x=1in different regions with N_1, Ec, γ.

	I	II	III	IV	V
Sh1	9.9637	10.0409	9.8288	8.6664	13.7017
Sh2	2.6029	2.6423	2.5312	1.9288	2.6817
Sh3	-4.957	-5.916	-4.840	-5.009	-7.344
α_1	$\pi/4$	$\pi/3$	π	2π	$\pi/4$
Sr	0.5	0.5	0.5	0.5	1.5

Table-6: Nusselt Number (Nu) at x=1in different regions with α_1, Sr.

5. CONCLUSIONS

The effects of radiation parameter, thermo-diffusion parameter, and dissipation on convective heat and mass transfer flow of a viscous chemically reacting electrical conducting fluid through a porous medium in a rectangular duct under the action of an inclined magnetic field. The important conclusions are

- The actual temperature at y=h/3, y=2h/3 levels, x=1/3 level it enhances with increases in the radiation parameter N_1 while at x=2/3 level it reduces with N_1. Larger the radiative heat flux smaller the actual concentration at y=2h/3,x=1/3 and x=2/3. while larger the actual concentration at y=h/3.An increase in N_1 enhances |Nu| on the lower and intermediate quadrants and diminishes on the uppermost quadrant with $N_1 \leq 1.5$ and higher $N_1 \geq 2.5$ enhances |Nu| on the lower quadrant and reduces on the intermediate and upper quadrants. The rate of mass transfer on all the three quadrants enhances with increase in N_1.
- The actual temperature reduces at x=1/3 and enhances at y = 2h/3 levels with increase in Soret parameter Sr while at x=2/3 & y=h/3, the actual temperature diminishes with rise in Sr≤1.0 and increases Sr>1.5 and|Sr|<0. The actual concentration diminishes with Sr<1 and enhances with higher Sr >1.5 at y=h/3 and x=1/3 levels. Also it reduces with |Sr|(<0) .At x=2/3 level the actual concentration reduces in the horizontal strip(0≤y≤0.33)

- and enhances in the region ($0.33 \le y \le 0.66$) with $Sr < 1.0$. For higher $Sr > 1.5$ and $|Sr|(<0)$ we notice an enrichment in the horizontal strip(0,0.33) and reduces in the region (0.33,0.66). At y=2h/3 level, it enhances with $Sr < 1$, reduces with $Sr > 1.5$ and $|Sr|$ (<0).The Nusselt number on first and intermediate quadrants increases with Sr and diminishes on the uppermost quadrant. The Sherwood number experiences an enhancement with Sr on all the quadrants.
- Greater the dissipative heat smaller the actual temperature at all levels. Higher the dissipative heat smaller the actual concentration at all vertical levels and at horizontal level y=2h/3 level .At y=h/3 level it enhances in the vertical strip ($0.33 \le x \le 1$).The rate of heat transfer reduces on the lower quadrant and enhances on the intermediate and upper quadrants with $Ec \le 0.03$ and enhances on all the quadrants with $Ec \ge 0.05$.Sherwood number enhances with Ec in lower quadrant, diminishes with $Ec \le 0.03$ and increases with higher $Ec \ge 0.05$ in middle quadrant while enhances with $Ec \le 0.03$ and reduces with $Ec \ge 0.05$ in upper most quadrant.
- An increase in the inclination α_1 of the magnetic field increases the actual temperature at y=2h/3 level and depreciates at all vertical levels and at horizontal level y=h/3. An increase in $\alpha_1 \le \pi/2$ leads to a depreciation in the actual concentration and enhances with higher $\alpha_1 \ge \pi$ at y=2h/3.At x=2/3&y=h/3 levels the actual concentration enhances and reduces at x=1/3 level with increase in α_1.The Nusselt number on all the three quadrants reduces with increase in $\alpha_1 \le \pi$ and enhances with higher $\alpha_1 \ge 2\pi$.An increase in the inclination $\alpha_1 \le \pi/3$ enhances $|Sh|$ and reduces with higher $\alpha_1 \ge \pi$ on all the three quadrants.

6. REFERENCES

1. J.D. Verschoor, P. Greebler, Heat Transfer by gas conduction and radiation in fibrous insulation, Transactions of the American Society of Mechanical Engineers. (1952**),** 961-968.
2. Y. Kamotani, L.W. Wang, S. Ostrach, H.D. Jiang, Experimental study of natural convection in shallow enclosures with horizontal temperature and concentration gradients, International Journal of Heat and Mass Transfer, 28(1)(1985**),** 165-173.
3. S. Ostrach, H.D. Jiang, Y. Kamotani, Thermo-solutal convection in shallow enclosures, Proceedings of the ASME-JSME Thermal Engineering Joint Conference, Hawali, 1987.
4. R. Viskanta, T.L. Bergman, F.P. Incropera, Natural Convection: Fundamentals, Hemisphere, Washington, D.C., (1985), 1075-1099.
5. A. Bejan, Mass and heat transfer by natural convection in a vertical cavity, International Journal of Heat and Fluid Flow, 6(3)(1985), 149-159.
6. J. Lee, M.T. Hyun, K.W. Kim, Natural convection in confined fluids with combined horizontal temperature and concentration gradients, International Journal of Heat and Mass transfer, 31(10)(1988), 1969-1977.
7. J.W. Lee, J.M. Hyun, Double-diffusive convection in a rectangle with opposing horizontal and concentration gradients, International Journal of Heat and Mass Transfer, 33(8)(1990), 1619-1632
8. P. Ranganatha, R. Viskanta, Natural convection of a binary gas in rectangular cavities, Proceedings of the ASME-JSME Thermal Engineering Joint Conference, Hawali, 1987.
9. O.V. Trevisan, A. Bejan, Combined heat and mass transfer by natural convection in a vertical enclosure, ASME J. Heat Transfer , 109,(1)(1987), 104-112.
10. O.V. Trevisan, A. Bejan, Mass and heat transfer by natural convection in a vertical slot filled with porous medium, International Journal of Heat and Mass Transfer, 29(3)(1986), 403-415.
11. C. Beghein, F. Haghighat, F. Allard, Numerical study of double – diffusive natural convection in a square cavity, International Journal of Heat and Mass Transfer, 35(4)(1992), 833-846.
12. T. Nishimura, M. Wakamatsu, A.M. Morega, Oscillatory Double-diffusive convection in a rectangular enclosure with combined horizontal temperature and concentration gradients, International Journal of Heat and Mass Transfer, 41(11)(1998), 1601-1611.
13. G.M. Oreper, J. Szekely, The effect of an externally imposed magnetic field on buoyancy driven flow in a rectangular cavity, Journal of Crystal Growth, 64(3)(1983), 505-515.
14. H. Ozone, M. Maruo, Magnetic and gravitational natural convection of melted silicon-two dimensional numerical computations for the rate of heat transfer, JSME, 30(1987), 774-784.
15. J.P. Garandet, T. Alboussiere, R. Moreau, Buoyancy driven convection in a rectangular enclosure with a transverse magnetic field, International Journal of Heat and Mass Transfer, 35(4)(1992), 741-748.
16. S. Alchaar, P. Vasseur, E. Bilgen, Natural convection heat transfer in a rectangular enclosure with a transverse magnetic field, ASME Journal of Heat Transfer, 117(3)(1995), 668-673.
17. N. Rudraiah, R.M. Barron, M. Venkatachalappa, C.K. Subbaraya, Effect of a magnetic field on free convection in a rectangular enclosure, International Journal of Engineering Sciences, 33(8)(1995), 1075-1084.
18. N.M. Al-Najem, K.M. Khanafer, M.M. El-Refaee, Numerical study of laminar natural convection in tilted enclosure with transverse magnetic field, International Journal of Numerical Mechanics Heat Fluid Flow, 8(6)(1998), 651-672.
19. M.A.H. Mamun, Md.T. Islam, M.M. Rahman, Natural convection in a porous trapezoidal enclosure with magneto – hydrodynamic effect, Non-linear analysis: Modelling and control, 15(2)(2010), 159-184.

20. M.M. Rahaman, R. Saidur, N.A. Rahim, Conjugate effect of joule heating and magneto hydrodynamic on double-diffusive mixed convection in a horizontal channel with an open cavity, International Journal of Heat and Mass transfer, 54(15-16)(2011), 3201-3213
21. M.M. Rahaman, F.Oztop. Hakan, A. Ahsan, J. Orfi, Natural convection effects on heat and mass transfer in a curvilinear triangular cavity, International Journal of Heat and Mass transfer, 55(21-22)(2012), 6250-6259.
22. Y.C. Ching, Hakan. F. Oztop, M.M. Rahman, A. Ahsan, M.R. Islam, Finite element simulation of mixed convection heat and mass transfer in a right triangular enclosure, International Communications in Heat and mass transfer, 39(5)(2012), 689-696.
23. M.M. Rahaman, F. Oztop. Hakan,; A. Ahsan, M.A. Kalam, Y. varol, Double-diffusive natural convection in a triangular solar collector, International Communications in Heat and mass transfer, 39(2)(2012), 264-269.
24. Hakan,F. Oztop, M.M. Rahman, A. Ahsan, M. Hasanuzzaman, R. Saidur, Ai-salem. Khaled, N.A. Rahim, MHD natural convection in an enclosure from two semi-circular heaters on the bottom wall, International Journal of Heat and Mass transfer, 55(7-8)(2012), 1844-1854.
25. P. Bera, V. Eswaran, P. Singh, Numerical study of heat and mass transfer in a anisotropic porous enclosure due to constant heating and cooling, Numerical Heat Transfer, 34(8)(1998), 887-905.
26. J.M. Hyun, J.W. Lee, Double-diffusive convective in a rectangle with cooperating horizontal gradients of temperature and concentration gradients, International Journal of Heat and Mass Transfer, 33(8)(1990), 1605-1617.
27. S. Kakac, W. Aung, R. Viskanta, Natural Convection – Fundamentals and Applications, Hemisphere, Washington DC, (1985),165
28. A.M. Morega, T. Nishimura, Double-diffusive convection by Chebyshev collacation method, Technological Reports of the Yamaguchi Univ.5, (1996), 259-276.
29. S. Strach, Natural convection with combined driving forces, Physicochemical Hydrodynamics, 1(1980), 233-247.
30. S. Acharya, R.J. Goldstein, Natural convective in an externally heated vertical or inclined square box containing internal energy sources, ASME Journal of Heat Transfer, 107(4)(1985), 855- 866.
31. A.G. Churbanov, P.N. Vabishchevich, V.V. Chudanov, V.F. Strizhov, A numerical study on natural convection of a heat-generating fluid in rectangular enclosures, International Journal of Heat and Mass Transfer, 37(18)(1994), 2969-2984.
32. K. Vajravelu, J. Nayfeh, Hydro-magnetic convection at a cone and a wedge, International Communications in Heat and Mass Transfer 19(5)(1992), 701-710.
33. Ali.J. Chamkha, Hydro-magnetic double-diffusive convection in a rectangular enclosure with opposing temperature and concentration gradients, Numerical Heat Transfer, 32(6)(1997), 653-675.
34. I.A. Badruddin, Z.A. Zainal, P.A. Aswatha Narayana, K.N.Seeth aramu, Heat transfer in porous cavity under the influence of radiation and viscous dissipation, International Communications In Heat & Mass Transfer, 33(4)(2006), 491-499.
35. A. Padmavathi, Finite element analysis of the Convective heat transfer flow of a viscous incompressible fluid in a Rectangular duct with radiation, viscous dissipation with constant heat source, Journal of Physics and Applied Physics, 2, (2009)
36. V. Nagaradhika, Y. Gatathri, D.R.V. Prasada Rao, A. Vasista, Convective heat transfer in a Rectangular cavity under the influence of radiation, viscous dissipation and temperature gradient dependent heat sources, International Journal of Electrical ,Electronic & Computing Technology, 2(4)(2011), 109-117.
37. G.Srinivas, Finite element of analysis of convective flow and heat transfer through a porous medium with dissipative effects in channel/ducts, Ph.D. Thesis, S.K. University, Anantapuramu, 2005**.**
38. M. Rangareddy, Heat and Mass transfer by Natural convection through a porous medium in ducts, Ph. D thesis, S.K. University, Anantapur, 1997.
39. S. Sivaiah, Thermo-Diffusion effects on convective heat and mass transfer through a porous medium in Ducts, Ph. D thesis, S. K. University, Anantapur, India, 2004.
40. G. Shanthi, S. Jafarunnisa, D.R.V. Prasada Rao, Finite element analysis of convective heat and mass transfer flow of a viscous electrically conducting fluid through a porous medium in a rectangular cavity with dissipation, International Journal of Electrical, Electronics& Computing Technology,2(4)(2011), 29-34.
41. Ali. J. Chamkha, Al-Naser Hameed, Hydromagnetic double-diffusive convection in a rectangular enclosure with opposing temperature and concentration gradients, International Journal of Heat and Mass Transfer, 45(12)(2002), 2465-2483.

Source of support: Nil, Conflict of interest: None Declared